NUMERICAL SIMULATIONS ON GRAVITATIONAL COLLAPSE [1]

Ioannis Taxidis

January 3, 2005

[1]This is a report of my work accomplished in the Astronomical Observatory of Copenhagen University, during my six - month stay in Copenhagen, in the framework of my participation to the European student - exchange program: SOCRATES - ERASMUS (October 2003 - April 2004). This work was supervised by **Prof. Åke Nordlund** (Niels Bohr Institute for Astronomy, Physics and Geophysics) and later on, by **Prof. Loukas Vlahos** (Aristotle University of Thessaloniki)

Contents

Chapter 1

Introduction

Starformation is one of the most important processes that modern astrophysics deals with. The birth of a star is a very complex phenomenon and a huge amount of work has been invested in order for scientists to be able to describe it, even in rough lines. Numerous observations of starforming regions, combined with analytical arguments and numerical experiments, compose our current understanding of the evolution of a molecular gas cloud, as it cools down and collapses under its own gravity, forming a single central core or a multiple system of cores which evolve into stars through the accretion of the surrounding gas.

Nevertheless we are still unable to describe with certainty the detailed evolution from the initial molecular cloud down to the final star, and there are numerous questions that have not been answered with clarity. How does the original cloud become fragmented and forms condensations? What are the properties of these condensations? When do they become gravitationally bound and begin collapsing under their own gravity? When exactly is the core created and what is the form of the infalling gas envelope around it? How is this envelope accreted onto it and what is the exact role of accretion phenomena such as accretion shocks and disks? How are magnetic fields affecting the whole process? How many stars will eventually be created and how much gas will finally end up on their surface? What are the properties of these final stars? For some of these questions and many similar ones, we are very close to a definite answer. Yet there are many left unanswered since we are still trying to figure out which factors are affecting each phase of the gravitational collapse and to what extent.

A very rough description of this kind of collapse is the following:
The initial cloud displays a non-homologous density distribution and in certain points some condensations tend to appear. Those on scales smaller than the Jeans length will eventually be smoothed out by acoustic waves, but large scale or very high density inhomogeneities, exceeding the Jeans length, will survive and grow in mass and size, resulting in the fragmentation of the cloud. Eventually, the gravitational forces acting on their surrounding gas, become much more important than the gas's self-gravity, leading to the halt of further fragmentation, and the collapse of the remaining material assumes the characteristics of

an accretion process. In the absence of any rotation, almost all the material around a core will end up on it, by following a motion that resembles free-fall. If there is substantial rotation, some part of the surrounding gas will form a rotating disk around the core, since it will probably not have enough time to loose its initial angular momentum. The evolution of such a disk is quite complex and a final theory has not been established yet. In any case, it is suggested that through the several angular momentum transferring processes that are known, a part of the disk will finally reach the central star while the rest will remain orbiting and will be the source of any subsequent planet formation.

The case of spherical collapse without rotation or magnetic fields is considered to be well understood and it has been followed analytically down to the formation of a central protostar. The exact description of the axisymmetric rotating collapse is much more complicated. The formation of a flattened disk rotating around its center is almost definite but its evolution appears to be hard to follow. One of the most important problems remaining still unanswered, is how the disk's angular momentum will be transferred outwards, so that the material becomes able to fall in the central core. The state of energy minimization for such a system has almost all the mass accumulated in the center, and only a small fraction left rotating, carrying all the gas's initial angular momentum. After all, this is more or less the picture of our solar system, where most of the mass is located in the sun and almost all the angular momentum is carried by the planets.

The mechanisms of angular momentum transport are, so far, poorly understood. The general idea is that friction between two disk particles, rotating at neighboring radii, will try to speed up the slower one and slow down the faster one. And since in most cases, the disk's angular velocity decreases outward, it follows that the inner particle will slow down, thus loosing part of its angular momentum and move inwards. On the other hand, the outer one will speed up and move to bigger radii. The net motion of angular momentum is outwards while the net motion of the disk mass is inwards, resulting to the disk accretion.

Since viscous transport processes are currently not well understood, many different possible mechanisms have been studied. Molecular viscosity appears to be too small to be effective enough. Turbulent convection was another possibility, but it has been suggested that it actually transports angular momentum inwards (Stone & Balbus (1996)). The most promising possibility so far is the "magneto-rotational instability", or "Balbus-Hawley" instability (Balbus & Hawley (1991)), where the stretching of the magnetic field lines due to different rotational velocities of neighboring annuli in the radial direction, causes the inner annulus to slow down and move inwards and the outer one to speed up and move outwards. Finally, another promising idea is the angular momentum transfer through gravitational instabilities that are created on the disk (Laughlin & Bodenheimer (1994)), provided that it has enough mass to be self-gravitating. In this scenario, some radially-extended mass condensations are created and they may form a spiral arm, rotating along with the disk. The inner part of the arm pulls the slower, outer one, trying to accelerate it, thus causing a net flow of angular momentum outwards. Naturally, in order for gravitational in-

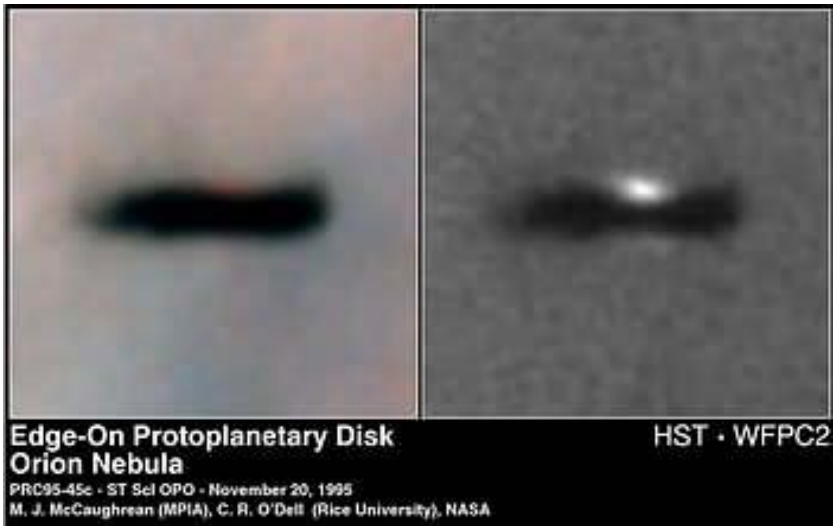

Figure 1.1: A thick dusty disk around a protostar in the Orion Nebula, seen edge on, through the Hubble Space Telescope. The left image is taken in blue, green, and red emission lines. The right image was taken through a different filter, which blocks any bright spectral emission lines from the nebula, and hence the disk itself is less distinctly silhouetted against the background. However, clearly visible in this image are nebulosities above and below the plane of the disk; these betray the presence of the otherwise invisible central star, which cannot be seen directly due to dust in the edge-on disk.

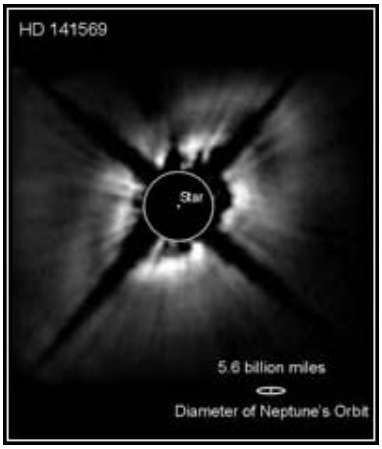

Figure 1.2: A striking NASA Hubble Space Telescope near-infrared picture of a disk around the star HD 141569,in the constellation Libra. Hubble shows that the 75 billion-mile wide disk seems to come in two parts: a dark band separates a bright inner region from a fainter outer region. The cause of this gap could be a planet.

stabilities to grow, the disk must have appreciable mass. All these mechanisms and more, are studied in order to appreciate which one (or which combination of them) is more efficient and realistic and produces the observed properties of the protoplanetary disks.

Most analytical arguments concerning the creation of a disk and its evolution have been tested through experiments, made with the use of numerical codes in one or more dimensions, according to the symmetry of the phenomenon. Unfortunately, the process seems to be quite sensitive to numerical methods and errors, since it is very hard to handle correctly properties such as numerical viscosity, diffusivity etc. Consequently, there is a rather vast variety of results, some of which were in agreement with analytical arguments, and others were the inspiration for further research.

It is useful to remind here, that although in most numerical simulations of rotating collapse, a disk does appear, its further evolution is still uncertain. How stable is this disk? Does it ever reach a Keplerian profile? Will it accrete most of its mass in the center? How much mass will remain orbiting? Note that the numerical experiments made by some researchers (Larson (1972), Black & Bodenheimer (1976)) describe the formation of a ring structure following that of a disk. They predict that this ring is unstable and will fragment into at least a binary system of condensations, orbiting around each other. Therefore there is still a great deal of uncertainty in the detailed description of gravitational collapse of even a very simple initial gas cloud.

Naturally, all this research at the analytical and numerical level has to be confirmed through astronomical observations. Numerous observations have been

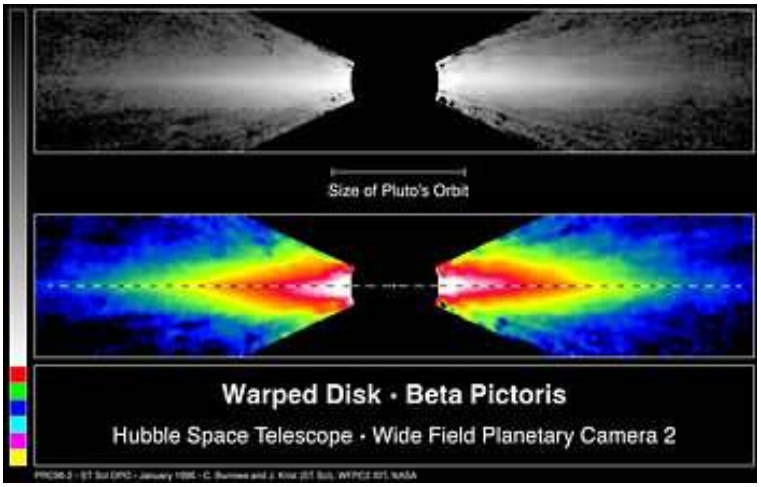

Figure 1.3: Optical image of an accretion disk surrounding the main sequence star Beta Pictoris. The bottom false-color image is applied through image processing and the inner edge of the disk is slightly tilted from the plane of the outer disk because of the possible presence of a planet.

made in starforming regions like the Taurus, Ophiuchus and Orion nebulae, which are the three most well-studied ones. Initially several attempts were made to detect protostellar cloud collapse by detecting directly the gas infall motions, but it has proven to be very difficult. The most general evidence for protostellar collapse is the detection of heavily-extincted infrared sources of low luminosity in starforming regions like the T Tauri stars. It has been proved that in the case of spherical collapse without rotation, were the infalling gas follows an almost free-fall motion, the protostars radiate most of their energy in the mid to far-infrared spectral region. Fortunately, NASA's IRAS satellite mission (launched in 1983) found many objects with spectral energy densities similar to those predicted by infall models. Disk formation in the rotating collapse cases is also supported by observations. Lynden-Bell & Pringle (1974) suggested that the excess near-infrared emission seen in many T Tauri stars could be powered by the accretion of dusty disks around the stars. Later on, it was proved that it could only be dust and not hot gas that causes this near-infrared emission. Therefore, dusty disks were the only plausible candidates for explaining the observed infrared spectra. The disk formation theories were later backed up by high spatial resolution imaging at optical and near-infrared wavelengths and by optical, near-infrared and infrared spectroscopy. The Hubble Space Telescope has recently given us some very impressive images of accretion disks around young stars (see Figures 1.1 - 1.3) so that the formation of disks in rotating, collapsing clouds is by now, undeniable.

In this project we present some numerical experiments, made with a 3-dimensional, hydrodynamical, numerical code (developed by Prof. Åke Nord-

lund), that simulate the gravitational collapse of several different cases of molecular clouds. We will deal with one spherical non-rotating collapse and three axisymmetric, rotating ones. The spherical case is the collapse of a singular isothermal sphere, where we make one simulation with a sink-cell in the center of the cloud, so that we can reproduce the self similar solution described by Shu (1977), and one without the application of a sink-cell in order to study its effects on the collapse. The next experiment sets the singular isothermal sphere in uniform rotation and examines the differences in the presence of significant rotation. Further on we observe the collapse of a rotating, spherical cloud with uniform initial density, where we can examine the first stages of the disk's evolution. We then repeat the same experiment with higher resolution in order to examine the effects of the boundaries. Finally we deal with the case of a non-axisymmetric rotating collapse where we initially have two layers of gas with different densities and rotational axes, so that we can see how the profile of the collapse changes when we move to more complex initial conditions. Throughout all these experiments, we set the temperature to be constant and we apply no magnetic fields at all. Wherever there is a specific analytical solution, we make the appropriate comparisons with our results. Our aim is to examine whether the theories which already exist predict similar results as the ones we get in our experiments, and to comment on the possible reasons for any differences observed.

Chapter 2

Numerical Method

Throughout all the experiments conducted, we have used the HD version of a 3D MHD numerical code in FORTRAN 90, developed by Prof. Åke Nordlund, called "stagger-code".

This code solves the standard MHD equations in the following form:

$$\frac{\partial \rho}{\partial t} = -\nabla \cdot \rho \mathbf{u}$$

$$\frac{\partial \mathbf{B}}{\partial t} = -\nabla \times \mathbf{e}$$

$$\mathbf{e} = -(\mathbf{u} \times \mathbf{B}) + \eta \mathbf{J}$$

$$\mathbf{J} = \nabla \times \mathbf{B}$$

$$\frac{\partial \rho \mathbf{u}}{\partial t} = -\nabla \cdot (\rho \mathbf{u}\mathbf{u} + \tau) - \nabla P + \mathbf{J} \times \mathbf{B} - g\rho$$

$$\frac{\partial e}{\partial t} = -\nabla \cdot (e\mathbf{u}) - P\nabla \cdot \mathbf{u} + Q_{cool} + Q_{visc} + Q_{Joule}$$

where ρ, $\mathbf{u}$, $\mathbf{B}$, $\mathbf{e}$, η, $\mathbf{J}$, τ, e, g, $P = (\gamma - 1)e = \frac{2}{3}e$, $T = p/\rho$, Q_{cool}, Q_{visc}, and Q_{Joule} are the density, velocity, magnetic field, electric field, electric resistivity, electric current, viscous stress tensor, internal energy, constant of gravity, gas pressure, temperature, cooling term, viscous dissipation and Joule dissipation respectively.

The variables are represented on staggered meshes, where in terms of a unit cube, ρ and e are volume centered, $\mathbf{B}$ and $\rho\mathbf{u}$ are face centered and $\mathbf{e}$ and $\mathbf{J}$ are edge centered. A sixth order accurate method, involving the three nearest neighbor points on each side, is used for determining the partial derivatives. The result is returned at a point which is shifted half a grid point up or down

relative to the input values. A fifth order accurate interpolation method, again involving the same six neighboring points, is used in order to shift the result into place. Artificial diffusion is handled through a technique similar to the one used by Richtmeyer & Morton (1964). The boundaries are set to be periodic and for evolving the MHD equations in time, the explicit 3rd order predictor-corrector procedure by Hyman (1979) is used, modified for variable time steps.

Chapter 3

Singular Isothermal Sphere

3.1 Theoretical Introduction

In the first experiment of this project, we deal with a non-rotating cloud. We examine the gravitational collapse of a gas sphere that initially has initial density profile $\rho \propto r^{-2}$ and no velocities at all.

There are numerous earlier publications on this subject, some dealing with it analytically and others using numerical HD codes. One of the most influential articles is that of F. Shu (1977), where he examines the collapse of an isothermal gas sphere whose initial density profile is:

$$\rho = \frac{c_s^2}{2\pi G} \cdot \frac{1}{r^2}$$

where c_s is the sound speed and G is the gravitational constant, so the mass enclosed in radius r, is increasing linearly as:

$$M_r = \frac{2c_s^2}{G}\, r$$

Shu is making a reference to earlier works by other scientists, which demonstrate that prior to core formation, collapse eventually leads to such an r^{-2} density profile of the cloud. He supports this claim with the argument that such a distribution of mass is as close as possible to mechanical balance. In order to be achieved, though, it is necessary that all the parts of the gas can communicate acoustically, meaning that the earlier phases of the gas flow should be subsonic.

From the moment this distribution is established, the gas sphere is in highly unstable equilibrium and with a small perturbation, starts to collapse. He examines this collapse analytically and concludes that it happens in a self-similar way. His main argument is that the time needed by each spherical cell to fall to the central core is approximately equal to its free-fall time:

$$t \approx t_{ff} \propto \frac{1}{\sqrt{<\rho>}} \propto r$$

and since $M \propto r$, it leads to $\frac{dM}{dt}$ =constant. So the accretion rate should be constant, and subsequently the core mass should increase linearly with time. Thus, after developing the HD equations in a self-similar manner, he describes the collapse as follows:

A spherical expansion wave is created, moving from the center outwards with the speed of sound ($r_w = c_s \cdot t$). The parts of the gas enclosed by the wave are falling freely towards the center. The outermost regions remain unaffected until the expansion wave reaches them, where they loose their pressure support (since the inner layers have begun collapsing) and start falling as well. The layers that are collapsing will have a density distribution as: $\rho \propto r^{-3/2}$ while their velocity profile has the form of the free-fall case: $u_{ff} \approx \sqrt{\frac{2GM}{r}} \propto r^{-1/2}$. Until this wave reaches the outer boundary the collapsing process is self-similar and the mass that reaches the center per unit time is constant, leading to a core mass that is increasing linearly with time.

This analysis is supported by the work of Boss and Black (1982) who used an 1-D HD code with 40 grid cells, and a sink-cell at the core, and reached the same conclusions.

We want to examine the same case, by making simulations with a full 3-D, HD, numerical code (stagger-code) at higher resolution, and to see whether we find similar density and velocity profiles. Therefore we make two experiments: In the first one, a sink-cell is applied in the center of the cloud, unlike the second case. Meaning that in the first experiment, the mass that reaches the center of the cloud is removed and placed in one central cell, thus separating the core region from the rest of the cloud (envelope). In this way, the gravitational effect of the core is retained while any other possible effects on the envelope are avoided.

3.2 Experiment With Sink Cell

We use an 100x100x100 grid points box, in the center of which, we implement a gas sphere with a radius of 50 grid points (the physical radius is scaled to range from 0 to 0.5). The initial density profile of the sphere is:

$$\rho = \rho_0[(r^6 + 1^6)^{1/6}]^{-2}$$

where $\rho_0 = 0.1$, which remains very close to r^{-2} even for small radii, but still flattens close to the center of the box. Thus, the total scaled mass inside the box is $M_{tot} = 0.758$ (as computed numerically). We also scale the gravitational constant, so that $G = \frac{25}{4\pi}$ in order to achieve an initial condition that is very close to hydrodynamical equilibrium. Finally, we apply a softening in the gravitational potential so as to avoid a singularity in the center. The code ran for 500 timesteps.

In Figures 3.1 to 3.4 are the plots of four similar quantities. The spherically averaged mass in each spherical cell (upper left panels), the spherically averaged density in each spherical cell in logarithmic scale (upper right panels), the mass

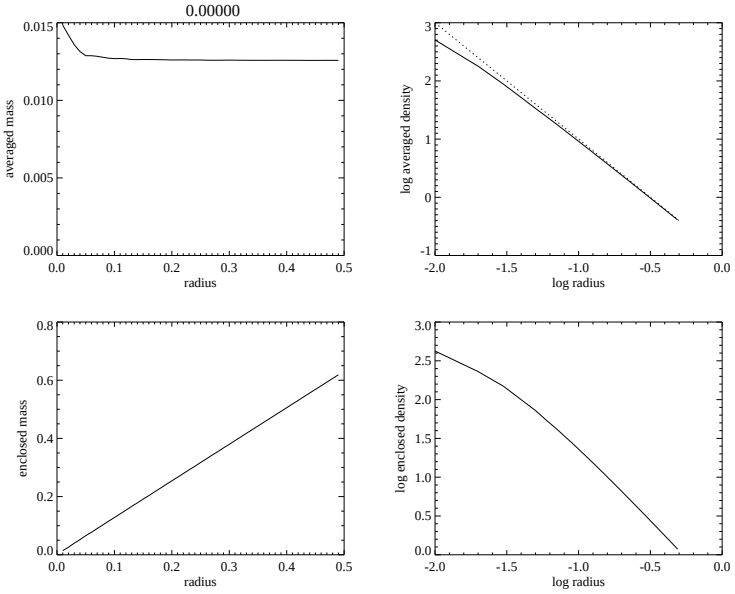

Figure 3.1: Spherically averaged mass (upper left panel), spherically averaged density in logarithmic scale (upper right panels), mass and density enclosed in each radial cell(lower left and right panels respectively). The dotted line in the spherically averaged density plots stands for r^{-2} power law, and the dashed one (see subsequent figures), for $r^{-3/2}$. Timestep=0

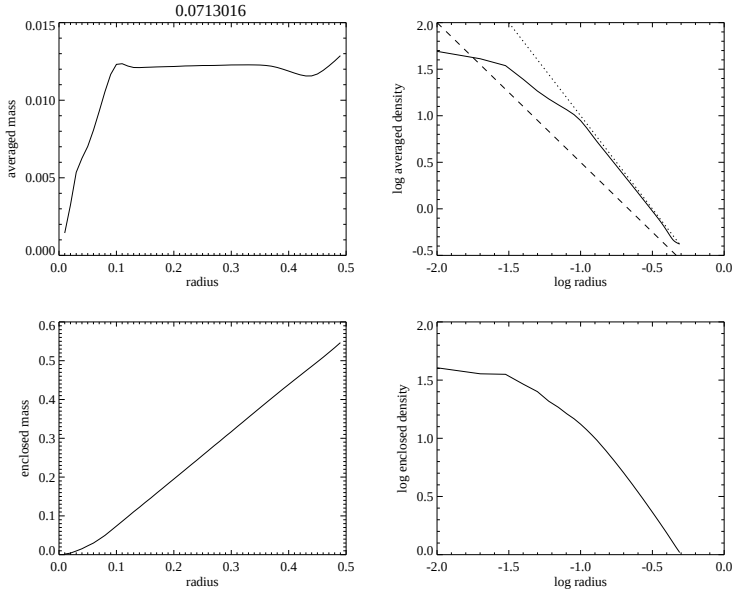

Figure 3.2: Same for timestep=250

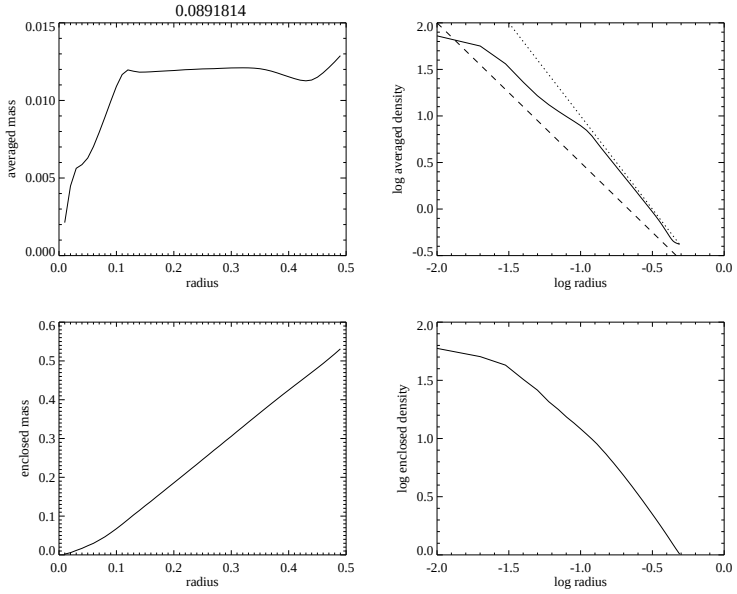

Figure 3.3: Same for timestep=350

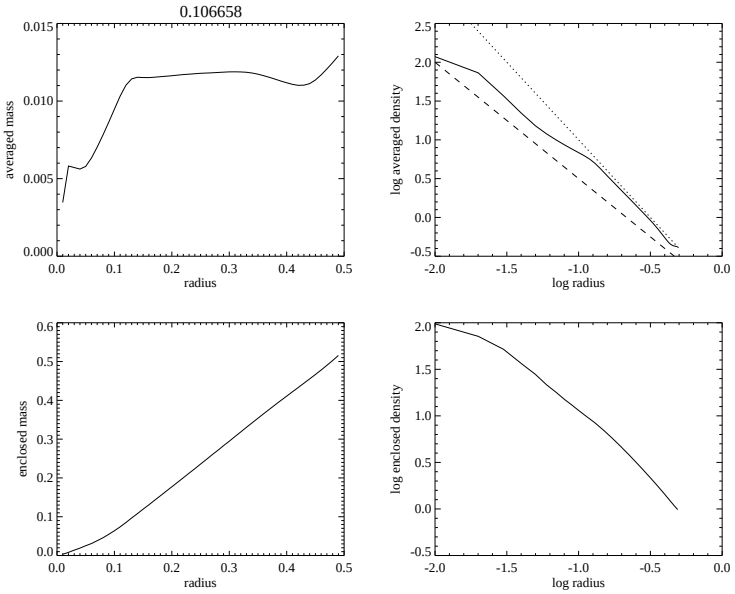

Figure 3.4: Same for timestep=450

and the density enclosed in each cell(lower left and right panels respectively). The dotted line in the spherically averaged density plots stands for the r^{-2} power law and the dashed one for the $r^{-3/2}$. The four timesteps plotted are timestep=0, 250, 350, 450. In each case, the physical scaled time is shown on top of the figure.

It is obvious that the initial density distribution is very close to r^{-2} and the enclosed mass ranges as: $M_r \propto r$. The mass in each spherical cell is naturally constant (Fig 3.1).

For $t \simeq 0.07$, the gas in the inner radii has already started to collapse as the expansion wave has reached $r_w \simeq 0.09$ (note that the sound speed is unity so the result is quite in agreement with $r_w = c_s \cdot t$). In later timesteps the wave is moving further out (Fig3.3 and 3.4), resulting in an increase of infalling mass. The density distribution of the collapsing gas is very close to: $\rho \propto r^{-3/2}$. Note though, that the mass which reaches the central core is put in the sink-cell, so that it has infinitesimal volume, not blocking the free-fall.

In Figures 3.5 to 3.7 are the plots of the radial velocity in logarithmic scale, for the previous timesteps (except of course for t=0). The dotted line represents the $r^{-1/2}$ power law. Although the wave is very clear, the velocity profile inside it has little resemblance with free fall. This is because free-fall is an ideal state and the velocity distribution appears more sensitive to diversions from this situation.

Finally we plot the central mass and accretion rate as a function of time, which can be seen in Figures 3.8 and 3.9. There we see, that after a peak

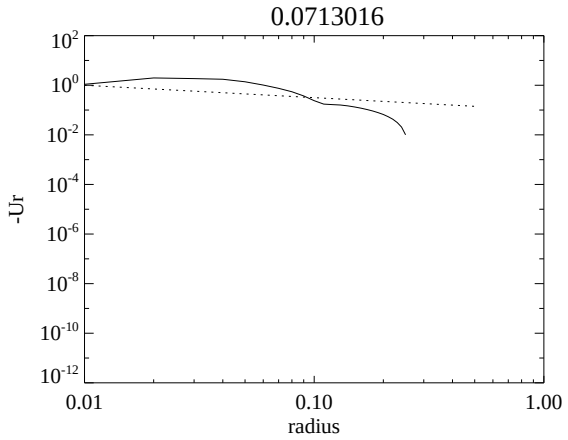

Figure 3.5: Radial velocity in logarithmic scale. Dotted line stands for $r^{-1/2}$. Timestep=250

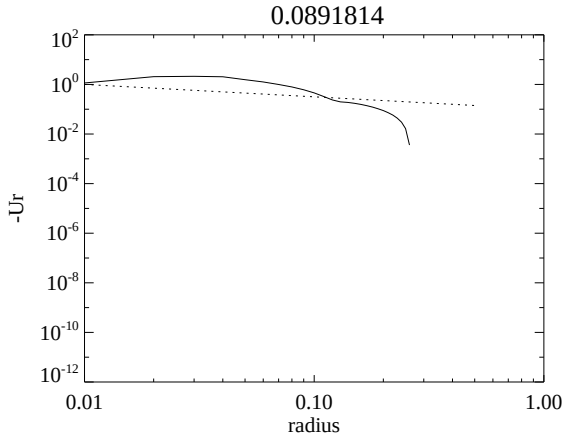

Figure 3.6: Same for timestep=350

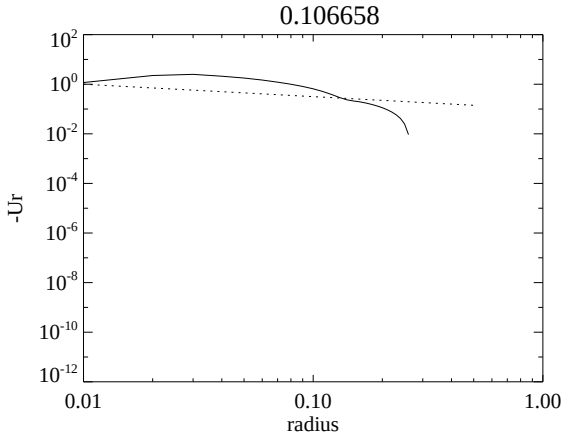

Figure 3.7: Same for timestep=450

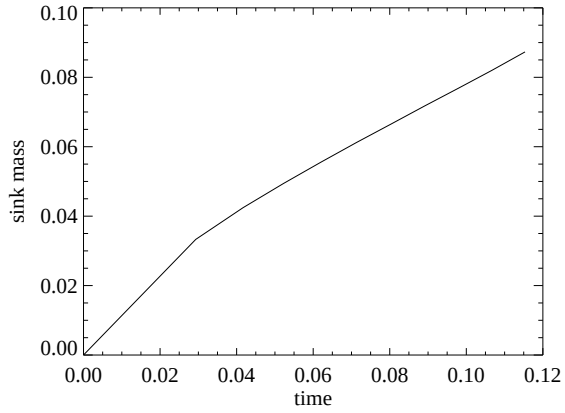

Figure 3.8: Central mass as function of time

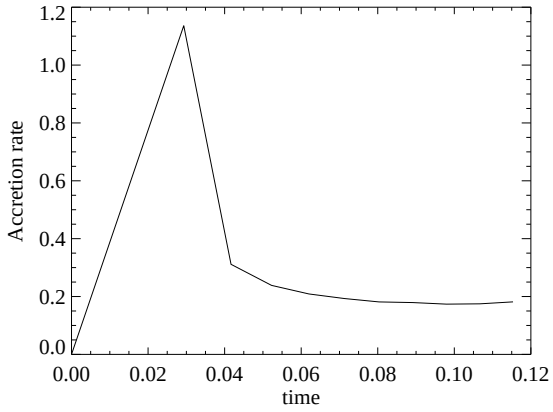

Figure 3.9: Accretion rate as function of time

in the accretion rate, it reaches a rather constant value of $\frac{dM}{dt} \approx 0.2$ and the sink particle mass grows linearly with time, thus verifying Shu's description of collapse in a qualitative way. The above results are also in close agreement with the numerical ones of Boss and Black, although extended in three dimensions.

3.3 Experiment Without Sink Cell

In the second experiment, the sink cell was not applied, in order for us to be able to examine what is the influence of the accumulation of mass close to the center in a core that has a certain volume. Here, the gravitational constant is set to $G = \frac{35}{4\pi}$, and the exact density profile is now:

$$\rho = \rho_0[(r^6 + 3^6)^{1/6}]^{-2}$$

The central softening in the gravitational potential is naturally still applied. This simulation ran for 1000 timesteps.

In Figures 3.10 to 3.13, the same mass and density variables are plotted as before, for timesteps: 125, 250, 500, 750 (Timestep 0 is practically the same as in Fig 3.1. Note that in timestep=125, the gas in a lot of spherical cells has already started to collapse, deviating from the initial distribution. In timestep=250, almost the whole cloud is collapsing, but still the collapsing regions have density distribution quite close to the $r^{-3/2}$ power law, which they retain even in later times. Yet, there seems to be no obvious expansion wave this time, and so the infalling layers are not well distinguished from the rest.

In Figures3.14 to 3.17 the radial velocity plots for each of the previous timesteps are presented. The deviation from the $r^{-1/2}$ power-law is obvious once more, since the velocity is increasing much faster as we move inwards. This is probably because there is pressure from the outer layers, acting on the

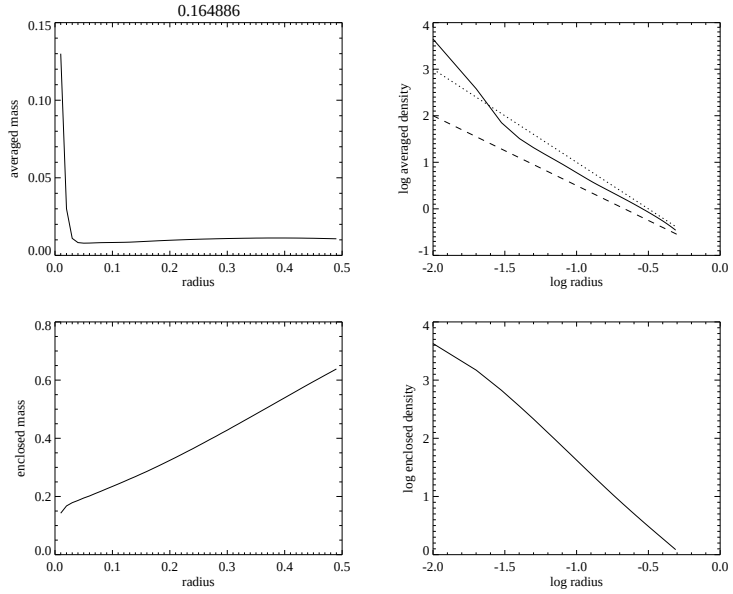

Figure 3.10: Same as in Fig3.1, but for the non sink cell case. Timestep=125

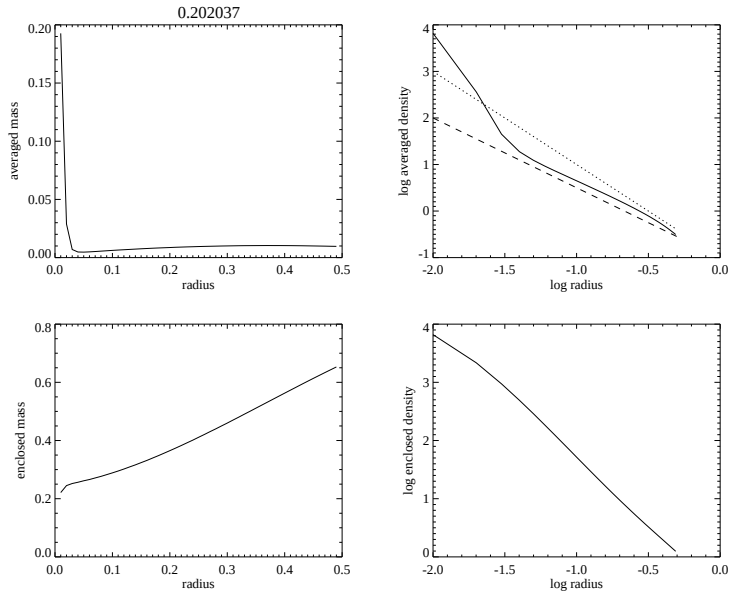

Figure 3.11: Same for timestep=250

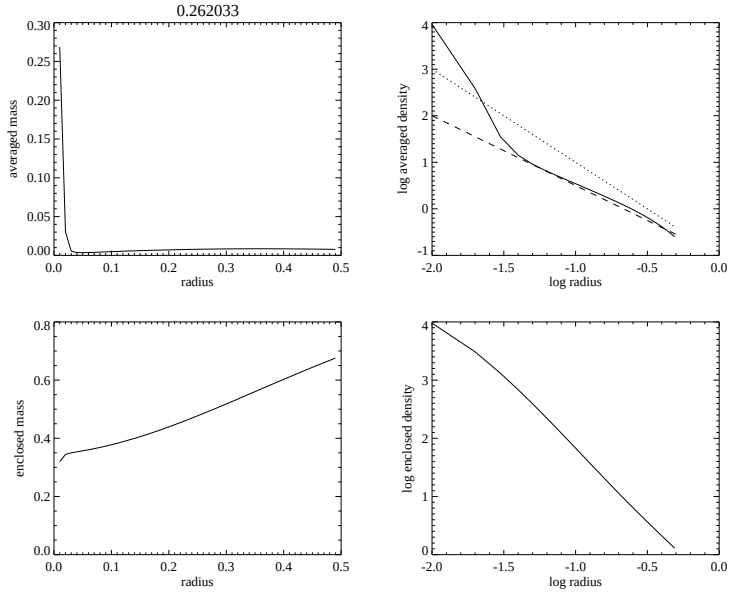

Figure 3.12: Same for timestep=500

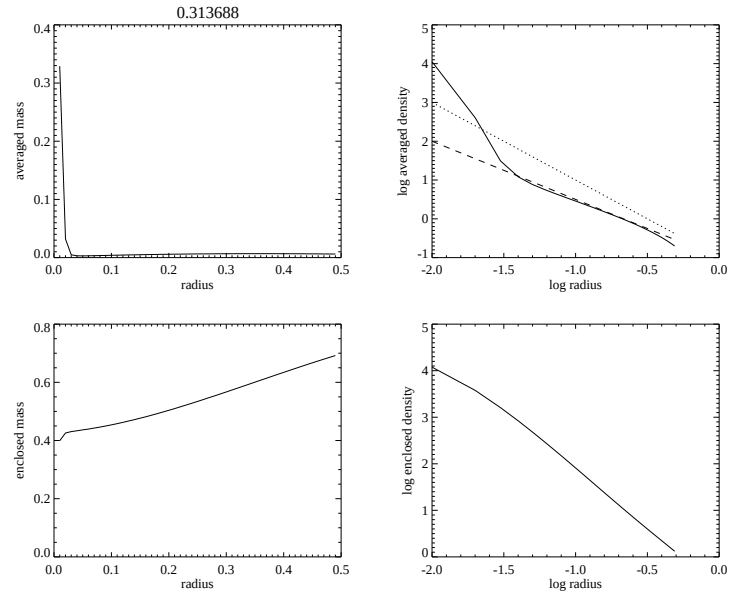

Figure 3.13: Same for timestep=750

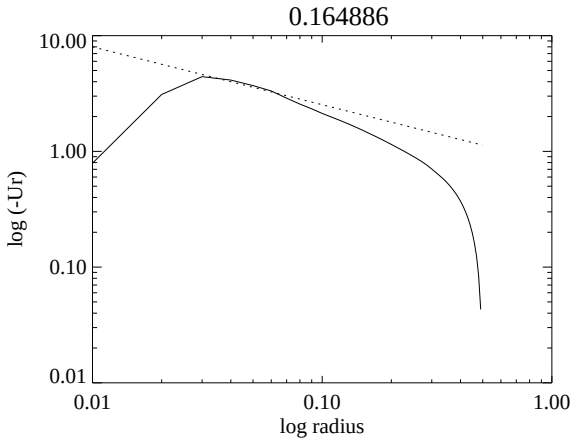

Figure 3.14: Radial velocity in logarithmic scale. Dotted line stands for $r^{-1/2}$. Timestep=125

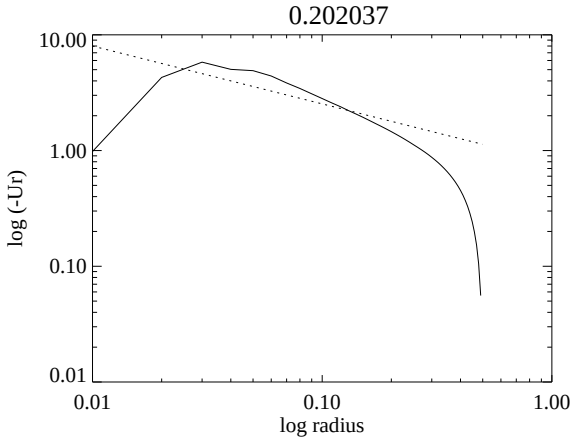

Figure 3.15: Same for timestep=250

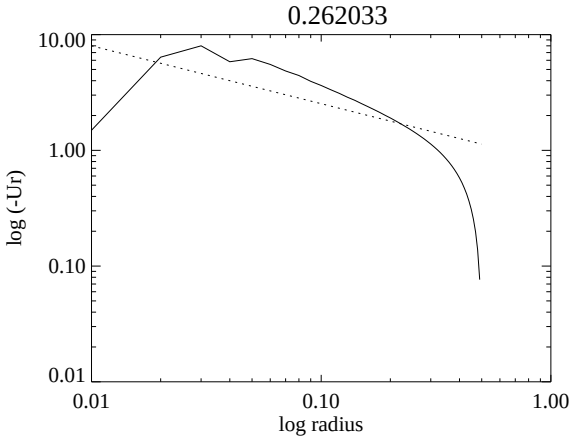

Figure 3.16: Same for timestep=500

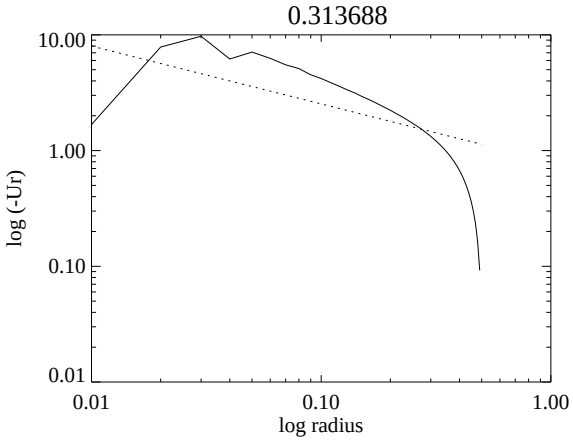

Figure 3.17: Same for timestep=750

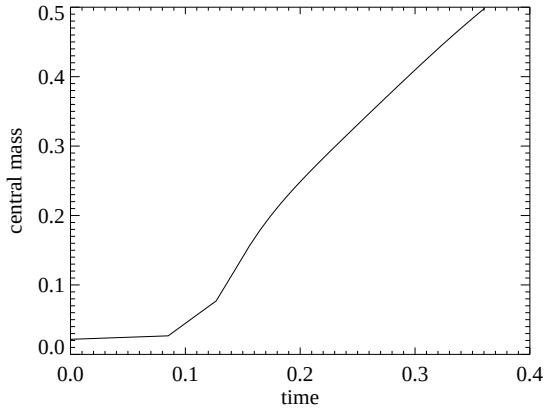

Figure 3.18: Mass accumulating at the central core as function of time

collapsing ones, and thus accelerating them more than gravitational acceleration. The equilibrium is destroyed from early times, which is natural, since the idealized case of the sink-cell does not apply here. The central core has a volume that is increasing continuously as matter is piling up on it, and the infalling material is dealing with increasing pressure from inside-out.

It is interesting to examine whether the constant accretion rate condition holds in this case. In Figures 3.18 and 3.19 the core mass and the accretion rate are plotted as functions of time (We assume that the core extends over the innermost three cells).

There is a very distinct peak in the early phase of the accretion rate, and after $t \approx 0.2$, it comes close to becoming quite constant for only a short period. Naturally, at this time, the core mass reaches an almost linear relation with time. Note that the mass accumulated in the center, in this case, reaches much greater values than in the sink cell case. This happens because most of the layers start falling in very soon and so, as mentioned before, the pressure exerted on the inner shells by the outer ones increases their inward acceleration, resulting in greater infall speeds and thus greater accretion rates.

We can conclude that in order to reproduce Shu's self-similar results, to a satisfying degree, we have to store the mass that has accumulated close to the center into an extremely small space, which is the sink-cell, so as not to prevent the collapse of the outer radii in any way. Otherwise, the deviation from self-similarity analysis very soon becomes important, and self-similar results can not be applied as a realistic model.

3.4 Conclusions

With the application of a sink-cell, we observe:

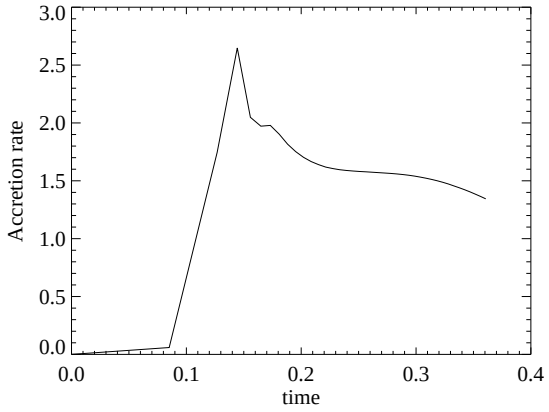

Figure 3.19: Accretion rate as function of time

- a spherical expansion wave traveling outwards
- density distribution close to an $r^{-3/2}$ power-law
- velocity distribution deviating from the expected $r^{-3/2}$ power-law
- accretion rate becoming constant after the first steps.

Without the application of a sink-cell:

- there is no distinct expansion wave. The equilibrium is soon lost and the whole cloud collapses.
- we do not observe the density and velocity distributions indicating free-fall
- the accretion rate is never stabilized.

Therefore, by applying a central sink-cell we can describe the singular isothermal sphere's collapse in terms of an almost free-fall state. But in a more realistic experiment we see that the volume and mass increase of the central core region is strongly affecting the procedure and the pressure forces that develop around this region can result in a big deviation from free-fall.

Chapter 4

Rotating Singular Isothermal Sphere

4.1 Theoretical Introduction

Having examined the case of the non-rotating, singular, isothermal sphere we continue with the same spherical cloud in which we now implement an initial rotation with uniform angular velocity (solid body rotation).

Cassen and Moosman (1981) used ballistic orbit analysis in order to describe the particles trajectories as a function of their initial angle with the rotational axis. Later on Tereby, Shu and Cassen (1984) expanded the self similarity solution of singular isothermal spheres (see Chapter 3) for slowly rotating cases, where they dealt with rotation as a small perturbation to the equations. Boss and Black (1982) also worked on this subject by using a 2D numerical code.

Firstly, we look at how a simplifying, theoretical analysis describes this collapse. Since the collapse is happening in dynamical timescales, it is unlikely that there will be enough time for the angular momentum to be efficiently transferred to the external medium. So the different parts of the cloud that are at a distance from the rotational axis, carrying substantial angular momentum, will start collapsing not towards the core itself, but towards the equatorial plane where they meet their symmetric particles coming from below. There they will collide and a shock wave will be produced, carrying their dissipated energy. So they will remain close to the equatorial plane forming a flattened structure i.e. a disk, that is rotating around the central core.

A specific particle that initially carries angular momentum L, which is conserved during its motion, will end up on this disk, in some final radius r_d around the center. There the centrifugal force will eventually counterbalance gravity, leading to the relation :

$$\frac{GM}{r_d^2} = \Omega^2 r_d = \frac{L^2}{r_d^3}$$

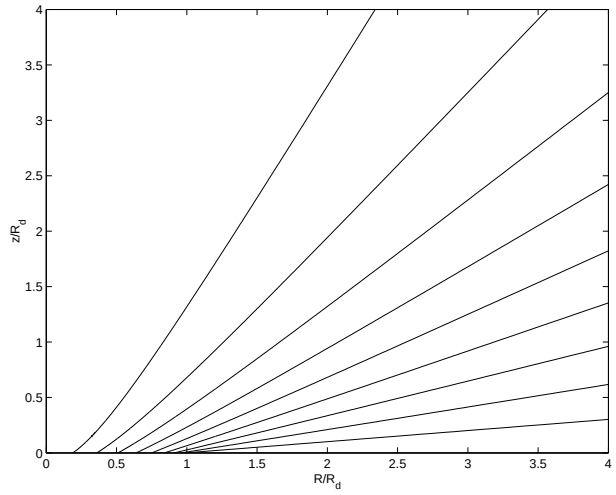

Figure 4.1: Streamlines of particles. Distance scales from the polar axis z and the cylindrical radius R are given in units of the final disk radius R_d. The streamlines shown are in steps of 0.1 in $cos\phi_0$ with the lowest streamline for $cos\phi_0 = 0.9$

So we can compute its orbiting radius :

$$r_d = \frac{L^2}{GM}$$

And since the initial angular momentum is equal to : $L = \Omega r_0^2 \sin^2 \phi_0$ (where ϕ_0 is the initial angle from the rotational axis) we can derive, that the bigger ϕ_0 is, the bigger the final radius will be. Therefore the material that is initially on the equatorial plane ($\phi_0 = \pi/2$), will finally have the biggest radius, corresponding to the disk's outer radius:

$$R_d = \frac{\Omega^2 r_0^4}{GM} \tag{4.1}$$

Note that in the analysis above we made two simplifying assumptions: That the pressures forces are negligible and that the whole mass of the cloud is accumulated in the center, meaning that the disk has no self gravity. In a more realistic analysis, those constrains should not hold a priori and the result could be quite different. From the moment the particle reaches its final orbiting radius, its rotational velocity will, theoretically, become a Keplerian one: $U_d = \sqrt{\frac{GM}{r_d}} = \frac{L}{r_d}$. Assuming that initially the cloud was rotating with a solid body rotation (which gives the constant Ω and the angular momentum profile $L_0 = \Omega r_0^2 \sin^2 \phi_0$), we can use ballistic trajectories, i.e. follow the particles parabolic motion around the central point mass (see Fig 4.1), and end up with

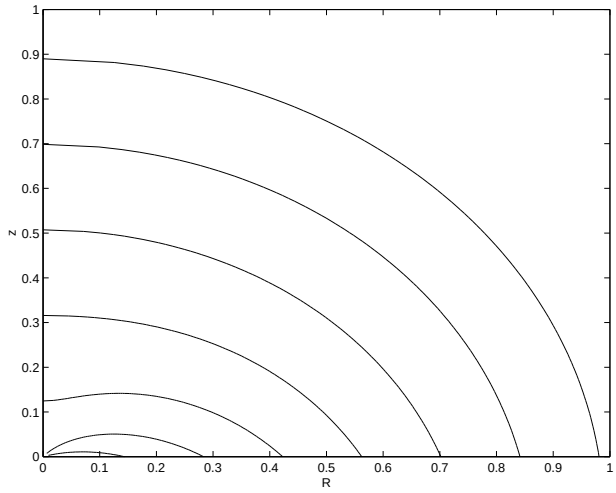

Figure 4.2: Density contours of equation 4.2. The flattening of the contours on the equatorial plane is evident

the equation for the density of the infalling material:

$$\rho = \frac{\dot{M}}{4\pi\sqrt{(GMr^3)}}(1+\frac{\cos\phi}{\cos\phi_0})^{-1/2}(\frac{\cos\phi}{\cos\phi_0}+\frac{2\cos^2\phi_0}{r/R_d}) \tag{4.2}$$

The density contours of this distribution become flat for small r, representing the creation of a disk. This is clearly depicted in Fig 4.2. For $r \gg R_d$ it becomes $\rho \propto r^{-3/2}$ (like in free-fall motion) while for $r \ll R_d$ it goes to $\rho \propto r^{-1/2}$. So as we move towards the center, the density should increase with a smaller rate, since rotation becomes preeminent and material is landing on the disk instead of the core.

Unfortunately, equation 4.2 is deduced after neglecting a lot of factors and making (perhaps too many) oversimplifying assumptions. Apart from the ones mentioned above, a basic simplification made is that for the occurring density distributions, we assumed that all the mass that is landing on the core (and comes mainly from the columns around the rotational axis where L is very small) is cramped in an infinitesimally small volume (like a sink-cell), so that it has only a gravitational effect and does not effect the rest of the cloud with its volume and the pressure forces that develop around it. In addition to that, in the distributions prementioned, the density of the disk itself is not included, since it is assumed to be infinitely thin and without self gravity. So finally the two density profiles correspond only to the infalling material. Another essential assumption is that the central accretion rate is constant, which leads us to the same conditions set by Shu's self similarity solutions for the non rotating isothermal sphere. This is exactly the reason why we get once more the free fall density profile: $\rho \propto r^{-3/2}$ for the outer shells, where the effects of rotation

can be neglected. Remember that in the same self similar analysis, the radius of the layers that begin collapsing is increasing linearly with time ($r_0 \propto t$) through the expansion wave ($r_w = c_s t$), and since $\dot{M}$ =constant$\Rightarrow M \propto t$, it is deduced from equation 4.1 that the disk's radius is related with time through eq. 4.1, as: $R_d \propto t^3$. Finally, note that for the ballistic analysis to be valid, the streamlines of the particles with different ϕ_0 must not intersect in any point of their motion, so that shocks will not be created and angular momentum can not be redistributed. That is the reason why we have to begin with solid body rotation where L is increasing monotonically with ϕ_0 meaning that the r_d does so as well.

4.2 Experiment

We have implemented the initial conditions for the rotating isothermal sphere, mentioned above, into the 3D stagger code, where naturally, the numerous constrains are not set beforehand, in order to examine whether the results will be in agreement with the theory.

The initial density profile is the same used in the previous section:

$$\rho = \rho_0[(r^6 + 1^6)^{1/6}]^{-2}$$

where $\rho_0 = 0.1$. The scaled angular velocity is set to: $\Omega = 4.9$ while we set $G = \frac{55}{4\pi}$ so that we have a ratio of rotational to gravitational energy

$$\beta = \frac{\frac{1}{2}L\Omega}{\frac{GM}{r_0}} = \frac{\Omega^2 r_0^3}{2GM} \approx 0.47$$

which is slightly less than the equilibrium value $\beta = \frac{1}{2}$ (where we assumed that all the cloud's mass is concentrated in the center. Theoretically, in order for the sphere to be close to HD equilibrium, having the Ω we set, it should be for the external layer ($r_0 = 0.5$):

$$GM = \Omega^2 r_0^3 \Rightarrow G \approx \frac{51.8}{4\pi}$$

Instead we set the slightly greater value mentioned, because there are pressure forces that have to be surmounted as well. So initially, the cloud is close enough to HD equilibrium. Note that once again we applied softening in the gravitational potential while a sink particle was not used. The box is 100x100x100 grid points where the scaled radius ranges from 0 to 0.5. The code run for 1000 timesteps.

Central mass and the accretion rate are plotted over time, in Figures 4.3 and 4.4 respectively. Until time $t \approx 0.1$ the mass in the central core is increasing quickly, thus resulting in the distinct peak in the accretion rate. This is mainly due to the collapse of the inner cells which are very close to the core, where the effect of rotation is negligible. But the violent increase of the core's mass

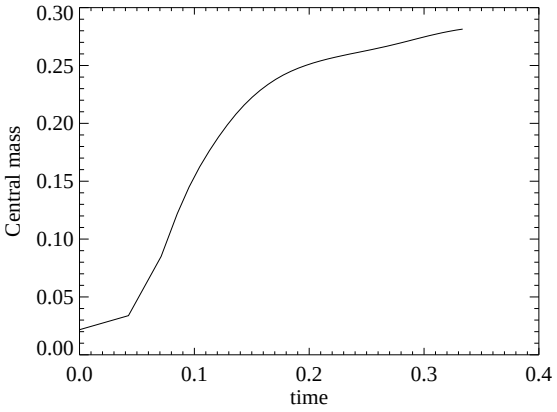

Figure 4.3: Mass accumulating at the central core as function of time

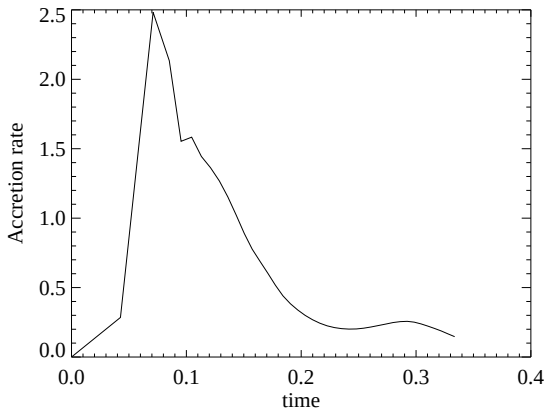

Figure 4.4: Accretion rate as function of time

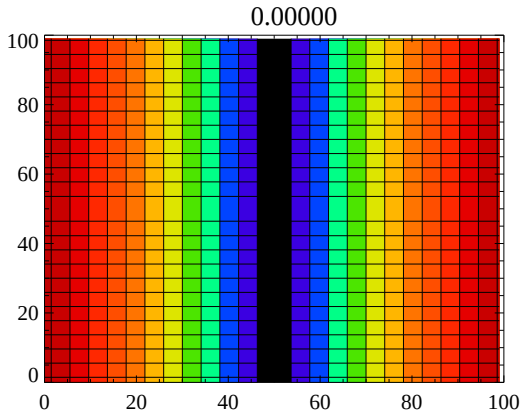

Figure 4.5: Contours of particles trajectories. Each column has a different specific angular momentum. The physical time is written on top. Timestep=0

should be mostly attributed to the collapse of the material close to the rotational axis. After this sudden increase, the accretion rate drops quickly, and gradually tends to 0, as one can also derive from the Fig 4.3 where the central mass tends to become constant. It is also remarkable that *the accretion rate has a very similar profile as the one acquired in the previous experiment* (see Fig 3.19). The distinct peak in the beginning has the same value (≈ 2.6) caused by the infall of inner layers, where rotation is negligible, and then drops by following a similar curve, thought with much lower values since most gas is now not falling directly to the core.

In Figures 4.5, 4.9 a slice of the box, passing through the meridional plane of the cloud, is depicted. The pictured timesteps are 0, 250, 500, 750, 1000. Each column corresponds to a different specific angular momentum and it is interesting to see how they are compressed by gravity near the equator, forming a flat disk around the center. The deformed columns in the final timestep essentially depict the trajectories followed by the particles and where they finally settled on the disk. By following each grid box one can see its initial and final location. Note that the trajectories do not seem to intersect. The dashed line in the final timestep represents the theoretical disk radius for a Keplerian disk, as given by Eq 4.1.

Looking at the plots of the rotational velocities along the equatorial plane in Figures 4.10 to 4.13 one can get a good impression of the disk rotational profile. The dashed lines correspond to Keplerian velocities (where we assumed that all the mass which affects the disk gravitationally is confined within the 5 inner radial cells). The velocities start as sub-keplerian but slowly increase with time as mass from the outer layers is accumulated on the disk, carrying greater L. The result is that the velocities become superKeplerian towards the final timesteps, which should result in the redistribution of mass and L. Note

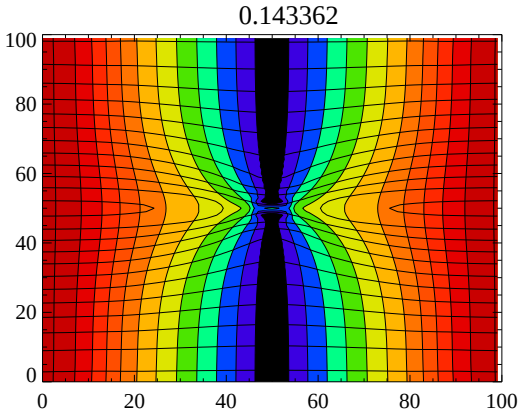

Figure 4.6: Same for timestep=250

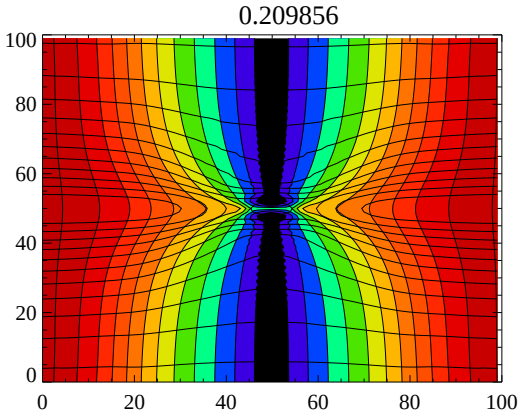

Figure 4.7: Same for timestep=500

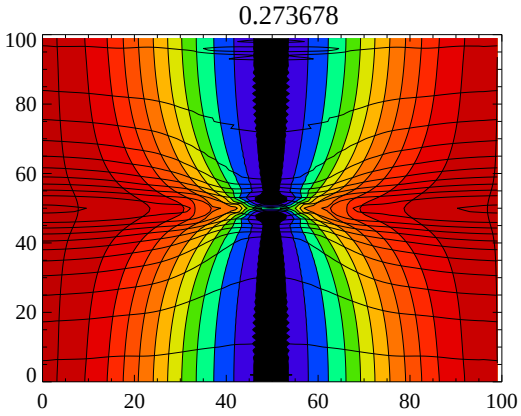

Figure 4.8: Same for timestep 750

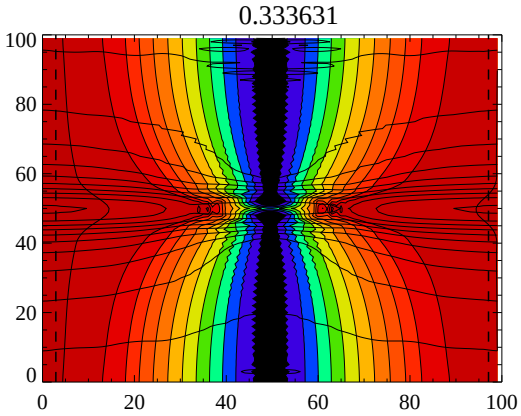

Figure 4.9: Same for timestep 1000

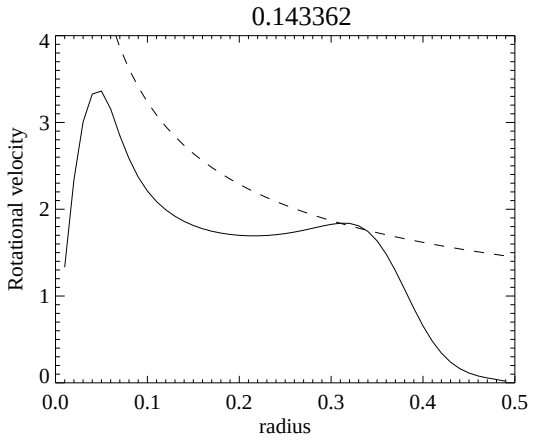

Figure 4.10: Rotational velocity over radius, on the equator. Dashed line stands for Keplerian rotation. Timestep=250

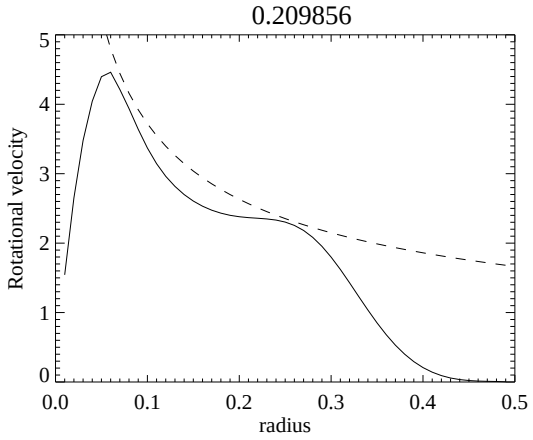

Figure 4.11: Same for timestep=500

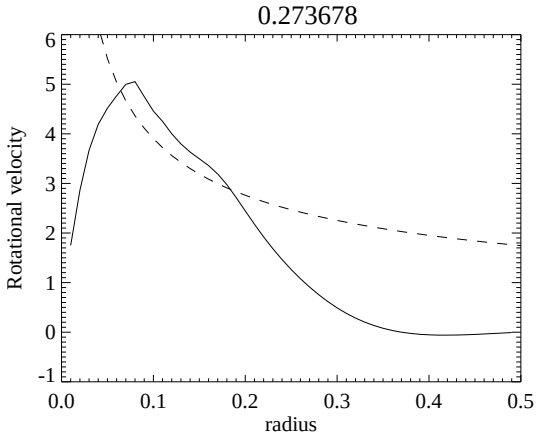

Figure 4.12: Same for timestep=750

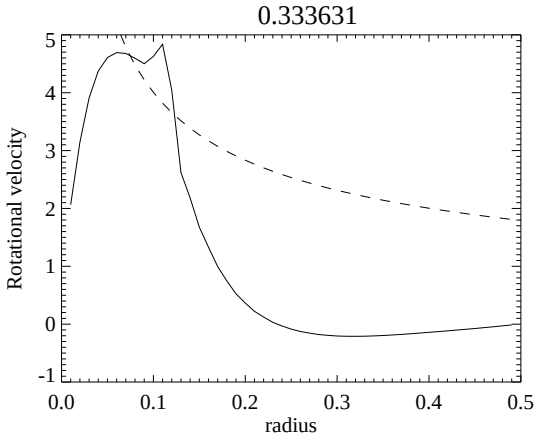

Figure 4.13: Same for timestep1000

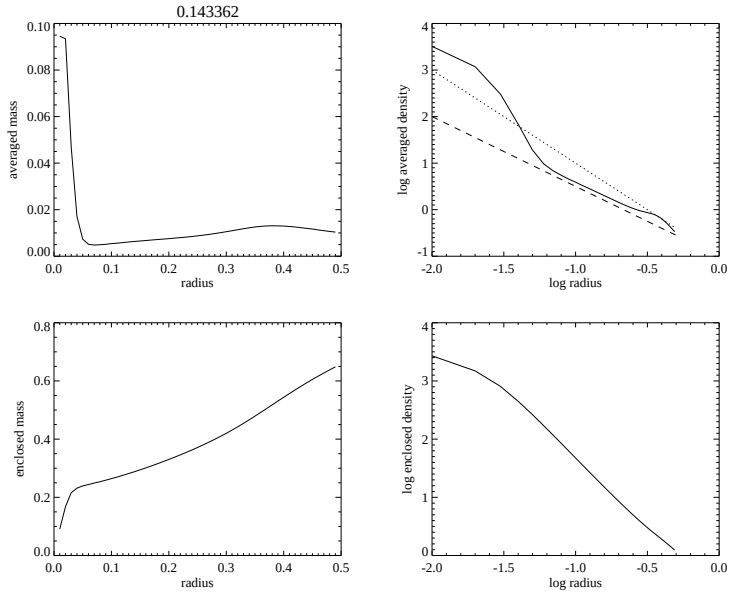

Figure 4.14: Spherically averaged mass (upper left panel), spherically averaged density in logarithmic scale (upper right panels), mass and density enclosed by each spherical cell (lower left and right panels respectively). The dotted line in the spherically averaged density plots, stands for r^{-2} power law, and the dashed one, for $r^{-3/2}$. Timestep=250

that only for a short period does the disk come close to being Keplerian, after which it looses its stability again.

In the density plots, in Figures 4.14 to 4.17, we can see how the inner shells that collapse first, form the core's mass, allowing the outer shells to start collapsing as well, acquiring a motion that seems close to free fall, since the density distribution resembles that of the power law $\rho \propto r^{-3/2}$ (dashed line). The layers that are close to the outer boundary show little motion and remain close to their original distribution. This image that resembles self similar solutions is soon lost, since the outer cells quickly start collapsing, carrying along their high angular momentum values and finally settling near the equator. From the plots of velocity or averaged mass, in timestep=1000, we can derive that the disk's radius is roughly $R_d \approx 0.15$. If the velocities were Keplerian like, and the orbits were stable, the radius could be derived from the angular momentum conservation:

$$\Omega r_0^2 = U_{kep} r_{kep} \Rightarrow r_{kep} = \frac{\Omega r_0^2}{\sqrt{\frac{GM}{r_{kep}}}} \Rightarrow r_{kep} = \frac{\Omega^2 r_0^4}{GM}$$

This formula of course, is the same as in Eq.4.1. Again we assumed that all the mass is accumulated in the core. So the Keplerian disk radius should be

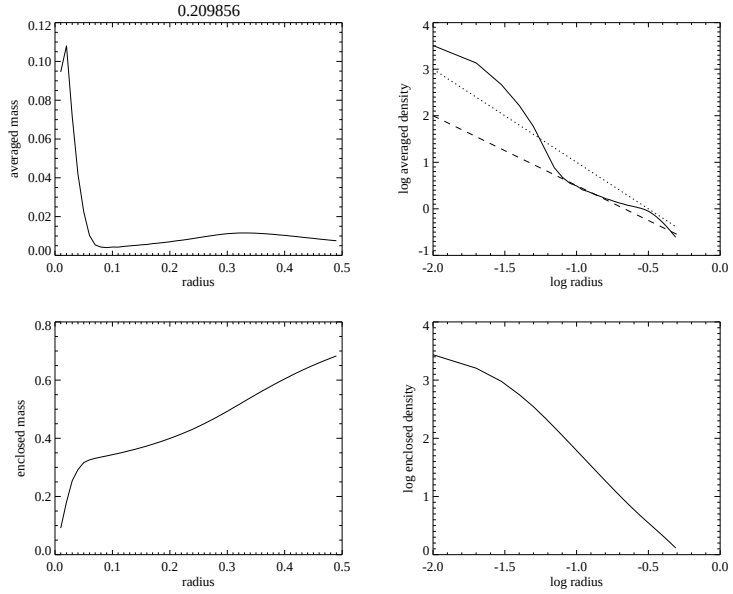

Figure 4.15: Same for timestep=500

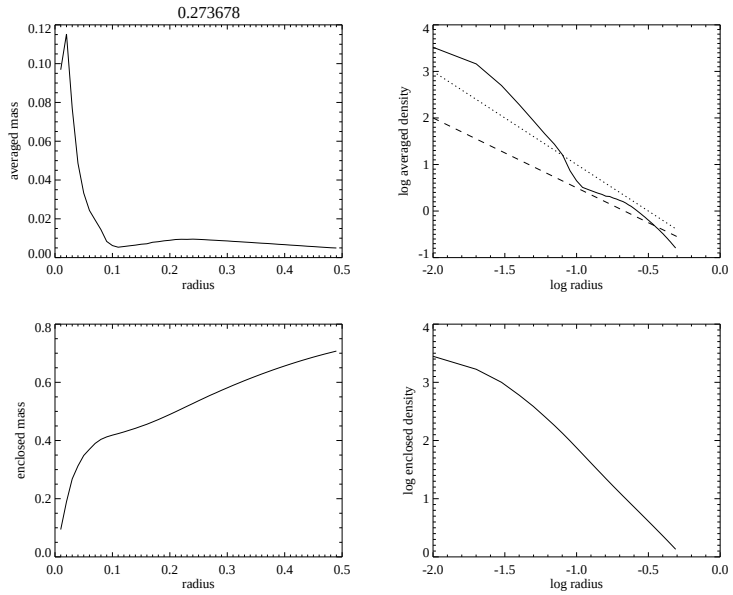

Figure 4.16: Same for timestep=750

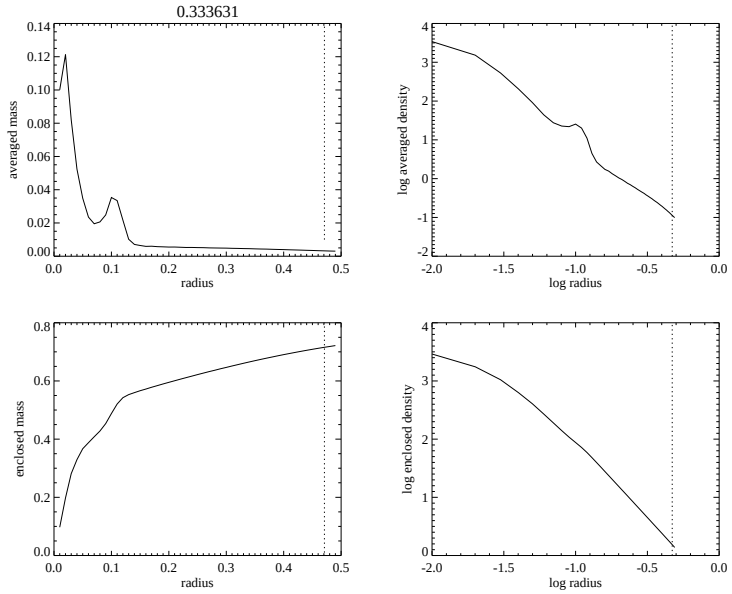

Figure 4.17: Same for timestep=1000

$R_d \approx 0.471$ which is shown as the dotted line in Figure 4.17. What we get though is a much smaller disk, since it never really managed to reach a stable Keplerian state and conserve it for long. Another reason for the divergence from the theoretical radius is that the theory does not take into consideration the pressure forces that develop both from the core towards the collapsing material and from the outer layers pressing the inner ones as they collapse. Finally one should note that the boundaries could also be affecting the outer layers.

Therefore we can conclude that although we started from a condition very close to HD equilibrium, and we did observe the main stages of the described process (central collapse of the inner shells, formation of disk), *the detailed evolution was totally differently from the theoretical one.* The collapse of the outer layers resembled self similar free fall only for a very small period in the beginning of the process, while we never found a distribution of $r^{-1/2}$ close to the core, since it didn't work as a sink-cell and the disk did not have a negligible mass. Finally, a main difference from the constrains set in the theoretical analysis, is that the accretion rate is very far from being constant in any time, and the pressure's effects can not be neglected at all.

As mentioned, Boss and Black (1982) applied an axisymmetric 2D HD numerical code on a similar initial condition, but their results were quite different. Naturally a disk was created in their experiments as well, but there was a circulation of gas on the disk, with material moving outwards, reaching the boundaries and then flowing away from the equator, only to join a flow towards the inner parts of the disk again. That kind of gas circulation was not observed in our

experiments. The gas moving outwards could be attributed to angular momentum redistribution, but the fact that it then returns to the disk is probably due to the boundary conditions. They also found a monotonically increasing accretion rate which is in total inconsistency with our experiment. But note that they applied a sink particle in the core thus excluding any significant pressure forces close to the center, and the effects of the mass as it piles up in the inner cells; effects that, according to our experiment, prove to be important in the evolution of the collapse. Finally take into consideration that they set the rotational-to-gravitational energy parameter to: $\beta = 0.1$, meaning that in their simulation, gravity was far exceeding rotation from the beginning, while in our case the clouds is initially close to equilibrium.

4.3 Conclusions

The theoretical analysis assumes the following simplifying conditions:

- the particles' trajectories do not intersect
- all the core mass is cramped in an infinitesimal space in the center of the cloud.
- the disk has no significant mass and thus no self-gravity as well
- there are no significant pressure forces
- the accretion rate is constant

In our simulation we have not implemented such simplifications. The results suggest that:

- truly the trajectories do not intersect significantly during collapse
- the core is not infinitesimally small. In fact, its size and most importantly the pressure forces around it are significantly affecting the collapse.
- the density distributions are not the expected ones. Only in the first steps do we observe one similar to free-fall density distribution. An $r^{-1/2}$ power-law is never reached by the infalling gas for $r \ll R_d$
- a rotating disk is observed as expected
- the disk did not acquire a Keplerian profile, therefore it never became stable
- the disk contains a significant portion of the cloud's mass, suggesting that its self-gravity should not be neglected
- the accretion rate is far from being constant at all times.

Chapter 5

Rotating Uniform Sphere

5.1 Theoretical introduction

In the same paper where they studied the collapse of a rotating singular isothermal sphere, Boss and Black also studied the case of an isothermal sphere with uniform initial density, rotating as a solid body. They describe the evolution as follows:

The collapse is occurring in roughly free fall timescales. The cloud starts collapsing at all radii but the core mass remains low, because there is no initial central concentration of mass like before. After some time, the core is massive enough to cause a violent runaway collapse, where the mass that is close to the rotational axis is falling freely inwards, while some material is accumulating on the equatorial plane. After a while, most of the gas has fallen into the core and there is a small part that was initially away from the axis, having large angular momentum, still rotating around it, in the form of a disk. The accretion rate now drops close to 0. The gravitational forces on the rotating gas are not enough to keep it from flowing outwards, so one part of it reaches the outer boundaries and stays there while the rest reaches a maximum radius and then is accreted again, partly reaching the core and partly reaching a stable Keplerian rotation. In the end only 5% of the initial cloud mass is left in the disk, unlike the centrally condensed cloud where the rotating gas was finally roughly 25% of the mass. Finally there are no circulation currents found in this case.

The main difference between these two cases is that in the uniform sphere, almost all the gas reaches the core! From a first point of view this might seem strange and one would expect the centrally condensed sphere to have less gas rotating around the core, since there is initially more central concentration of gas. Note though, that in the singular sphere the rotational to gravitational forces ratio is:

$$\gamma_{sing} = \frac{\Omega^2 r}{\frac{GM}{r^2}} = \frac{\Omega^2 r^3}{GM} = \frac{\Omega^2 r^3}{G\int 4\pi\rho r^2 dr} = \frac{\Omega^2 r^3}{G4\pi\rho_0 \int dr} = \frac{\Omega^2 r^3}{G4\pi\rho_0 r} = \frac{\Omega^2 r^2}{4\pi G\rho_0}$$

while in the case of the uniform density sphere the same ratio is:

$$\gamma_{un} = \frac{\Omega^2 r^3}{G4\pi\rho_0 \int r^2 dr} = \frac{\Omega^2 r^3}{G4\pi\rho_0 \frac{r^3}{3}} = \frac{3\Omega^2}{4\pi G\rho_0} = \frac{3}{r^2}\gamma_{sing}$$

Therefore as $r \to \infty$ the ratio becomes: $\gamma_{un} \ll \gamma_{sing}$ indicating that for the same angular velocity, the gravitational forces will be much stronger than the rotational ones when the cloud has a uniform density profile ($\rho = \rho_0$) than when it has a centrally condensed one ($\rho = \frac{\rho_0}{r^2}$). This is why the rotational effects in the uniform sphere are milder and the core accretes more mass.

5.2 Experiment

We want to study the same case by applying the HD version of the 3D stagger code. We use a 100x100x100 box in the center of which we implement a spherical cloud with constant scaled density $\rho = \rho_0 = 1$ which extends up to $r \approx 0.3$, beyond which it abruptly drops to 0, leaving its surroundings almost empty of gas. We also set an initial constant angular velocity: $\Omega \approx 9.5$. Therefore by setting $\gamma = \frac{3\Omega^2}{4\pi G\rho_0} = 1$ (rotational forces equal to gravitational in any radius r) we can compute the required value of G:

$$G = \frac{3\Omega^2}{4\pi\rho_0} = \frac{270.76}{4\pi}$$

Therefore we set $G = \frac{300}{4\pi}$ which proves enough to counterbalance both rotation and the pressure forces, in the first timesteps. With this values, the final radius of a Keplerian disk that has all the cloud mass concentrated in the center, is

$$R_d = \frac{\Omega^2 r_0^4}{GM} = \frac{3\Omega^2 r_0}{4\pi G\rho_0} \approx 0.27$$

and the ratio of rotational to gravitational energy is

$$\beta = \frac{\Omega^2 r_0^3}{2GM} = \frac{3\Omega^2}{8\pi G\rho_0} \approx 0.45$$

(β for rotational-gravitational balance would be $\beta = \frac{1}{2}$) indicating that gravity has only a small dominance over rotation. Having set these values we let the code run for 2000 timesteps. The evolution observed is the following:

Initially, the gas near the poles of the sphere is collapsing while the gas on the equatorial plane is moving outwards since gravity is not yet enough to surmount pressure and rotation. After some mass from the rotational axis has reached the core, gravitational forces are great enough for the equator to start contracting again, rather rapidly, pushing the infalling gas from the poles, outwards. Soon though, gravity takes over in all shells and the whole cloud is contracting. The material near the axis that was pushed out is accreted again and the gas that has enough angular momentum gradually approaches the equatorial plane. The

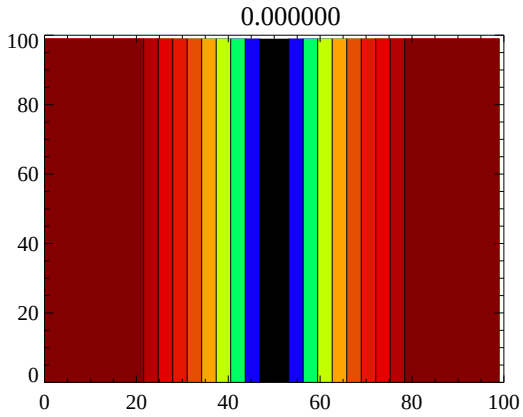

Figure 5.1: Contours of particles trajectories. Each column has a different specific angular momentum. Timestep=0

result is the formation of a thick disk around the core, where gas is gradually settling down near the equator. From timestep $\approx$ 1000 up to 1250 the core-disk system reaches a quite stable condition. By now, some material that was originally ejected towards the boundaries is returning, carrying some angular momentum and when it reaches the disk, four distinct arms are formed; but generally the disk's stability does not seem to be severely disrupted by this effect.

Once more we use contours where each column has a different value of specific angular momentum, in order to depict this process as clearly as possible. In Figures 5.1 to 5.5, the snapshots are plotted at timesteps 0, 500, 750, 1000, 2000 respectively, with the scaled time written on top of each Figure.

By $t \approx 0.225$, the gas close to the equator has begun forming the thick disk, while the parts near the axis are rapidly collapsing to the core, increasing the gravitational energy of the rotating parts. As time goes by, more gas is landing near the equatorial plane carrying high values of L. In the last timestep, the effects of the material that bounced on the periodic boundaries and then mixed with the rest of the gas are evident, as the homogeneity of the collapse is destroyed. The bouncing gas is mixed with the rotating layers, creating some turbulence while redistribution of L is occurring through the viscous torques that are developing. Yet, the disk structure remains, and its outer radius is in the last snapshot $R_d \approx 0.20$, which is a value quite close to the theoretically predicted for Keplerian disks.

We now examine the evolution of the central mass and the accretion rate as a function of time, shown in Fig 5.6 and 5.7. The central mass is initially increasing rapidly as gas from the inner shells with low rotational energy and most importantly, gas near the axis, is accreted, resulting in the distinct peak in the accretion rate. Later on, the rate is dropping as the outer layers land

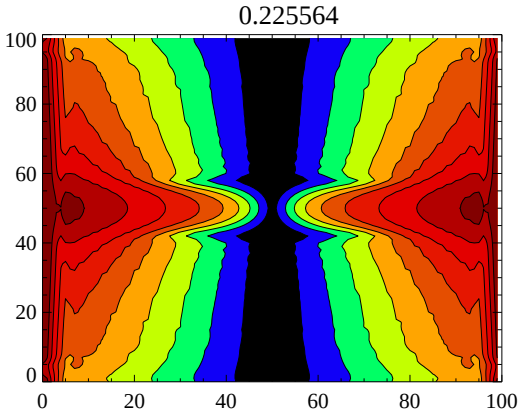

Figure 5.2: Same for timestep=500

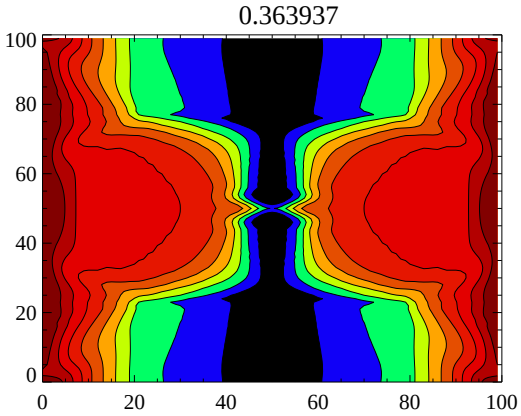

Figure 5.3: Same for timestep=750

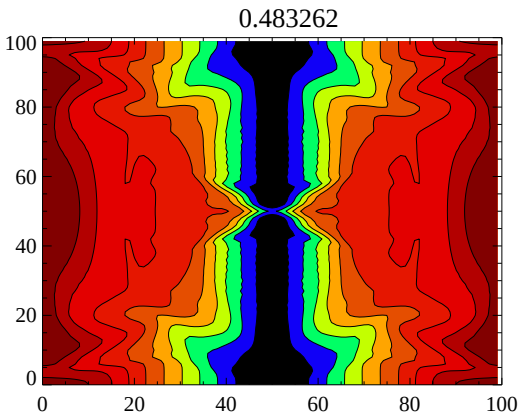

Figure 5.4: Same for timestep 1000

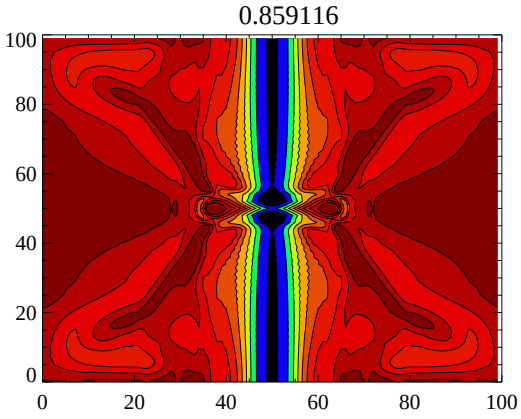

Figure 5.5: Same for timestep 2000

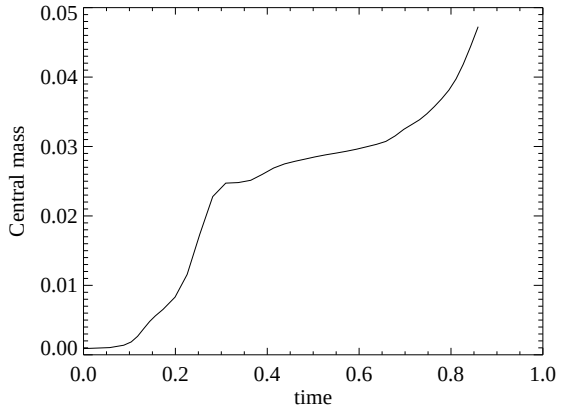

Figure 5.6: Mass accumulating at the central core as function of time

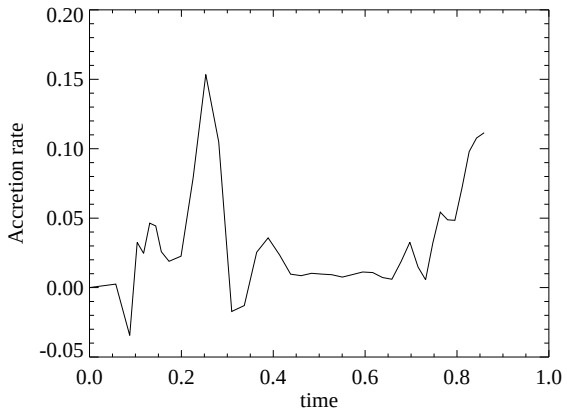

Figure 5.7: Accretion rate as function of time

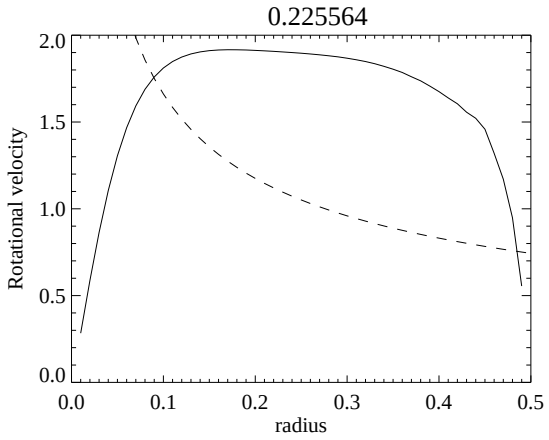

Figure 5.8: Rotational velocity on the equator, over radius. Dashed line stands for Keplerian rotation. Timestep=500

on the disk rather than the core. But although, after some point ($t \approx 0.65$), the majority of the rotating gas has reached the equator, the redistribution of mass and angular momentum is continuing, resulting in mass leaving the disk and falling into the core, thus increasing the accretion rate once again. A closer study of this redistribution is done below.

After examining more thoroughly the structure of the thick disk that has formed, one easily notices that it actually surrounds a thin quasi-Keplerian disk which extends over the equatorial plane and the planes close to it. It is this thinner disk that represents the most stably rotating part of the gas. Naturally, as its mass and total angular momentum are increasing by the accumulation of particles from the outer shells, it soon starts to decline from its Keplerian profile. These remarks are more clearly depicted in Figures 5.8 to 5.11, where the rotational velocities of the equatorial plane are plotted over radius. The dashed lines stand for Keplerian velocities profile of each timestep, where we assumed that the mass which acts as a gravitational center is the mass accumulated in the inner 5 shells. Note that another reason why the Keplerian profile is totally lost by the final timesteps could be the gas that reaches the disk from the boundaries, pressing it inwards, altering the quasi-equilibrium state that the Keplerian part of the thick disk had reached.

So, although we expected most of the gas to end up in the core, finally we find large amounts still rotating around it. Therefore we can conclude that independent of the initial density profile of the cloud, a disk is more or less bound to appear, were all the gas's angular momentum is stored. This disk will become stable when most of the gas reaches Keplerian orbits, but it does not seem very possible that it will be able to retain this profile for more than a few timesteps, since further accumulation of mass and energy dissipation through viscous processes will probably alter its structure.

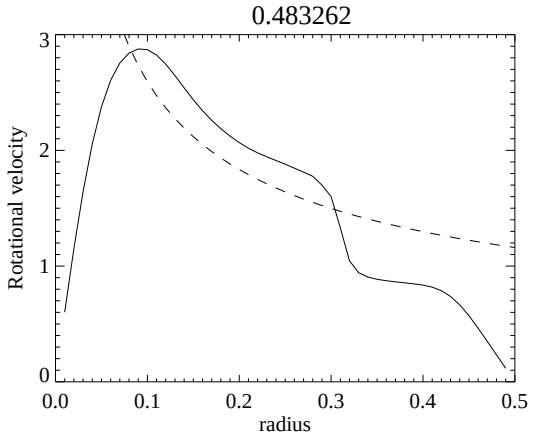

Figure 5.9: Same for timestep=1000

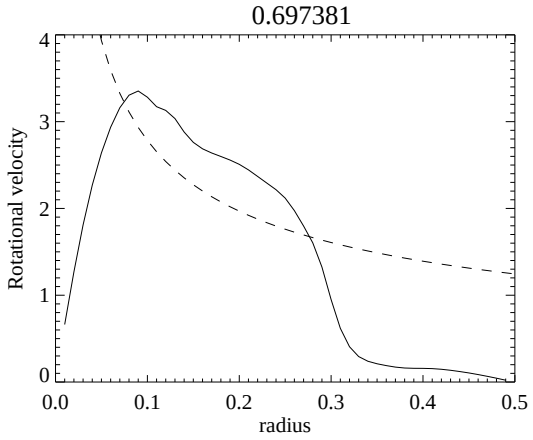

Figure 5.10: Same for timestep=1500

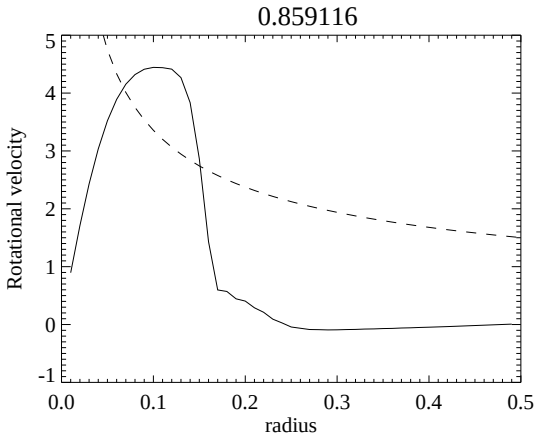

Figure 5.11: Same for timestep 2000

We now elaborate further on the subject of the redistribution of mass and angular momentum. When the particles settle on the disk or around it, the only way for them to end up in the core is to loose their angular momentum through some mechanism. These mechanisms are mostly viscous and magnetic torques that will dissipate energy (see Introduction). Since we have not set any magnetic fields in our experiments we will only study the first case. Between neighboring fluid parcels that rotate in slightly different radii, torques will develop because of their kinematic viscosity. These torques will cause the transport of angular momentum from the inner parcel to the outer one, causing the inner one to loose its rotational energy and move inwards. Theoretically, the final state of such a system would have all the mass having lost its angular momentum and fallen in the core, and only a very small amount of material, remaining in orbit at large radii, carrying all the angular momentum the cloud initially had. Of course this is a totally idealized situation, and an interesting question is how much mass will *actually* be wasted in carrying all the angular momentum?

Figure 5.13 shows the circularly averaged angular momentum per unit mass, of the gas rotating on the equatorial plane, plotted against radius. Several timesteps are depicted. It is obvious that most of the specific angular momentum is transported outwards during the first timesteps when the gas near the equator was moving outwards. The part of this gas that remained close to the boundaries has retained these high values of specific angular momentum that decreased only slightly throughout the whole run. On the other hand, the values of angular momentum in the inner shells are continuously increasing due to the settling of material arriving from the outer ones.

Further on, we plot the spherically averaged angular momentum (not angular momentum per unit mass) over radius. Specifically it is the spherically averaged specific angular momentum, multiplied with the average of the mass enclosed within each spherical cell ($< L >=< M >< L_{permass} >$). The plot is shown in

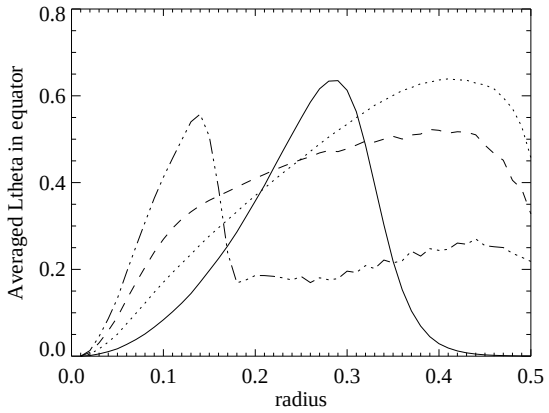

Figure 5.12: Angular momentum per unit mass, averaged over circular cells, on the equatorial plane. The timesteps are 0 (solid line), 500 (dotted line), 1000 (dashed line) 2000 (dashed-dotted line)

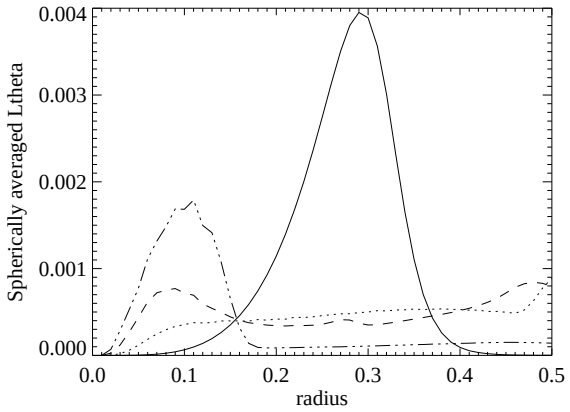

Figure 5.13: Spherically averaged angular momentum over radius. The timesteps are 0 (solid line), 500 (dotted line), 1000 (dashed line) 2000 (dashed-dotted line)

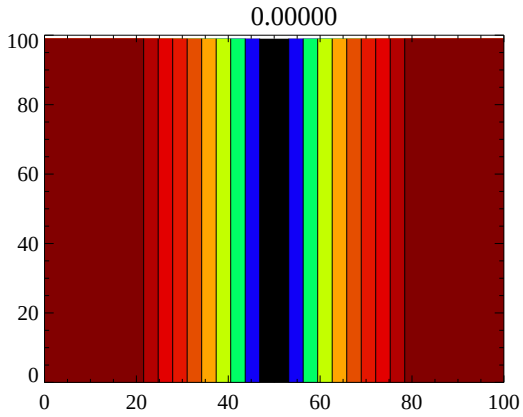

Figure 5.14: Contours of particles trajectories. Each column has a different specific angular momentum. Timestep=0

Figure 5.13 for the same timesteps as before. There we can see that although almost all the angular momentum is carried by gas contained in the disk, there is mass left rotating close to the boundaries, carrying some part of the initial L.

5.3 Experiment with higher resolution

From both the latter plots it is clear that the initial expansion near the equator, which ejects gas to the boundaries, has a significant effect on the results. The gas that returns from the boundaries is altering the disk's structure as it mixes with it, through the four arms that are formed. Some mass is left rotating close to the boundaries which is also making quite unclear whether there is any angular momentum transport from the inner parts of the disk to the outer cells. In order to elaborate further on this collapse, and also diminish these drawbacks, we rerun the same experiment, but within a bigger box. We implement the same sphere with the same rotation, in a 200x200x100 box, in order for most of the gas near the equator not to reach the boundaries (we needn't use more grid points in the z direction since the gas close to the rotational axis is accreted from the beginning). The only difference between this experiment and the previous one is that we have now set the sound speed to be equal to 0.5, while up until now, it always had the normalized value of 1. This means that the information of the density evolution is transported with half the speed it had before, thus altering the pressure effects. The code run for 1500 timesteps and the collapse is shown in Figures 5.14 to 5.19, where again each column corresponds to a different value of specific angular momentum and one can see the particles' trajectories.

Since this time, the gas has enough space to expand without reaching the boundaries and bouncing there (except for a very small fraction), the evolution

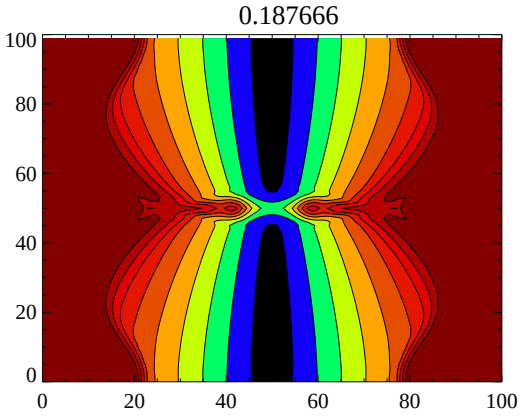

Figure 5.15: Same for timestep=250

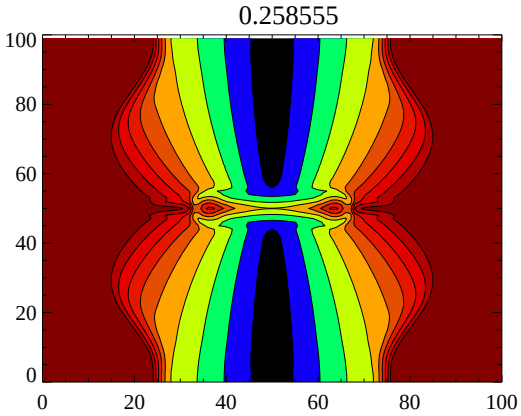

Figure 5.16: Same for timestep=500

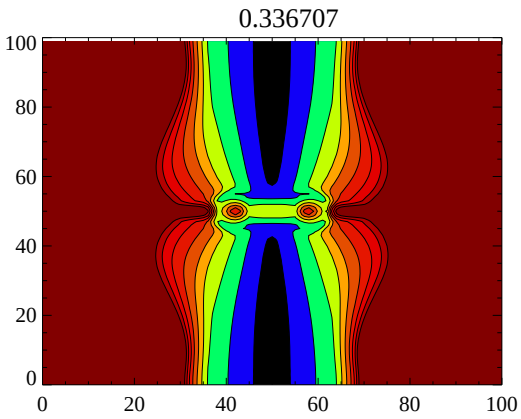

Figure 5.17: Same for timestep=750

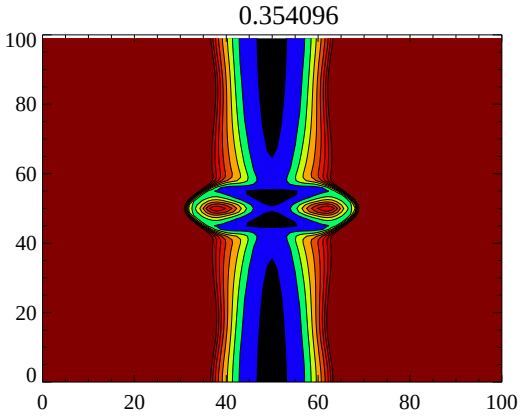

Figure 5.18: Same for timestep 1000

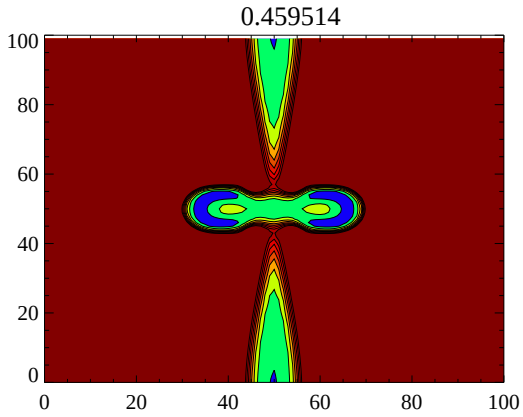

Figure 5.19: Same for timestep 1500

we observe is quite different. Once again the cloud's equator is initially expanding due to lack of efficient gravity, until most of the material from the axis has reached the core. Then it starts being accreted again and the equatorial plane contracts. A disk structure is soon emerging as the rotating gas is landing on it (Fig 5.15). Yet the pressure forces on the central part of the cloud appear now to be too strong, and as a result gas is *leaving* the core, while another part is still falling in from outer shells. This combination of pressure that drives the inner gas outwards, gravity that drives the outer parts inwards and rotation that spins the whole system creates an unstable flat structure on the equator that initially was disk-like but as time passes, eventually forms a *ring*. Now most of the mass is concentrated on this ring (Fig 5.16), at a distance from the core, and most of the infalling, rotating gas is landing on it. The ring is expanding since gravity seems to be inadequate to counterbalance rotational energy and pressures. Soon this unstable ring reaches a maximum radius which retains for a few timesteps and then contracts again, under its own gravity (Fig 5.17). After a while it looses its structure once more, and four spherical gas clumps form, which rotate around the center (Fig 5.19). (The fact that structures like the gas clumps in this experiment or the arms in the previous one, are always four, is due to the symmetry of the cubic box). Any gas that was left rotating is now accreted on these clumps, increasing their mass. This process is more clearly depicted in Figure 5.20 where density is plotted, in logarithmic scale, over the equatorial plane for timesteps 0, 500, 1000, 1500. There, the four stages of the process are obvious: uniform sphere, accretion disk, accretion ring, spherical gas clumps.

We can see that when the cloud is not tightly bound by boundaries, that more or less help it acquire a stable profile, but on the contrary, when it is free to expand in space and evolve under its own gravity and pressure, different structures occur. The evolution is much more complex as the gravity forces

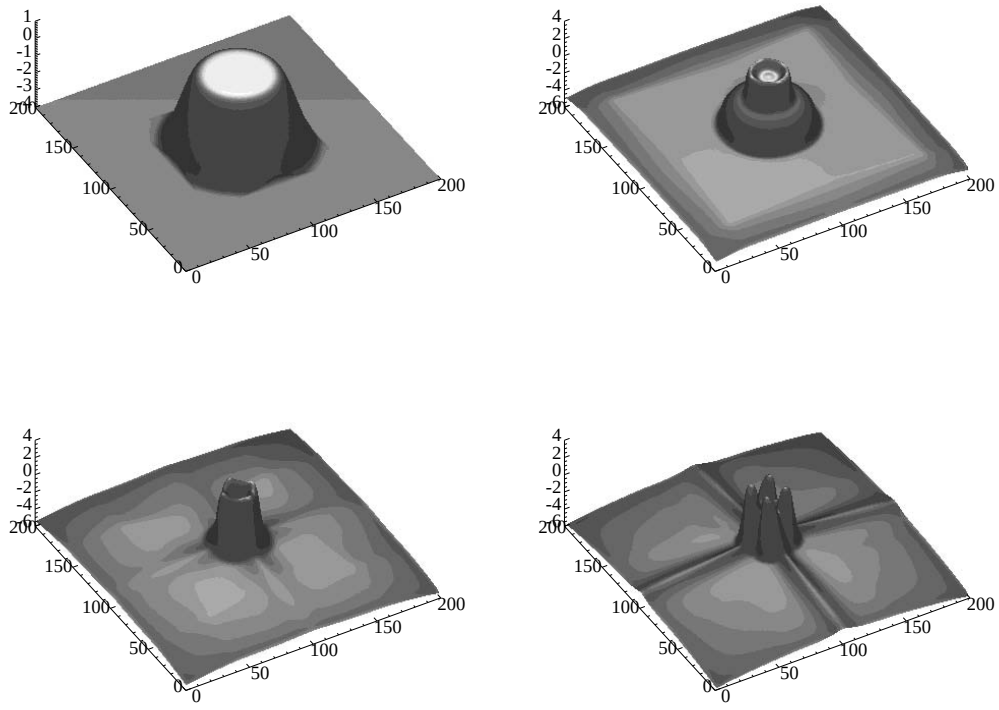

Figure 5.20: Logarithm of density on the equatorial plane. The physical, scaled times are 0.000, 0.258, 0.354, 0.459

are not always enough to surmount the very high pressures that develop in the central region. In addition to that, rotational energy is another factor that makes the case even more complicated.

In the previous experiment, where the box was smaller, the sphere followed a more simple and predictable path, where part of the gas reached the core forming a robust gravitational center, while the rest settled on a disk around it. Eventually, some of this disk's mass ended up in the core, and the rest remained in a rotational state carrying the angular momentum the cloud initially had. Theoretically we would expect most of the gas to reach the core, since in the case of the uniform sphere, the gravitational forces dominate the rotational ones, and this dominance grows with time as more mass reaches the core, mainly from the axis. Yet the disk managed to accumulate a great amount of the mass, (actually there is much more gas left rotating than in the core), indicating that either the particles that initially had a lot of angular momentum had not enough time to loose it, or that the viscous mechanisms, responsible for carrying angular momentum outwards, are not efficient enough. It appears though, that the fact that the sphere was contained within a small volume helped it evolve more normally. The gas that was initially in the equator and was ejected outwards, reached the boundaries very soon, there it met its symmetric parts from the exactly opposite side (since periodic boundaries are applied) which are rotating in the opposite direction. The viscous forces that developed dissipated its rotational energy hence the gas was driven back into the cloud pushing the disk inwards and causing it to decline from its quasi-Keplerian profile. The importance of this effect on the cloud's collapse is somewhat doubtful since most of the gas never reached the boundaries in the first place. In this latter experiment though, where the cloud had adequate space to expand, it appears that this factor was crucial. Yet, another factor that could also affect the different evolution observed in this last experiment is the reduced sound speed.

As it can be seen in Figure 5.21, the averaged specific angular momentum is evolving in a totally different way. This time the mass located close to the center is gradually *loosing* angular momentum though material is landing on it. On the other hand, the regions outside the ring have particles with angular momentum that is monotonically increasing with time. This feature is indicating that major quantities of angular momentum are being transferred outwards as some gas is leaving the disk (and later the ring), carrying high values of L with it. These particles will, eventually, reach the boundaries. Also the pressure forces appear to be determining, to a great extent, the way angular momentum will be distributed on the various radial cells and therefore the fate of the collapse itself. The high pressure that arises in the core soon counterbalances gravity, allowing the rotational forces to carry material outwards and to form a ring instead of a disk. But the circulation of angular momentum is continuing, with gas settling on the ring from above and below, carrying L with it, while some particles that developed great velocities are leaving the ring near the equator, thus decreasing its total specific angular momentum. This fact, along with the viscous forces that develop, finally results in the fragmentation of the ring into the four spherical clumps that rotate around the center. So instead of one

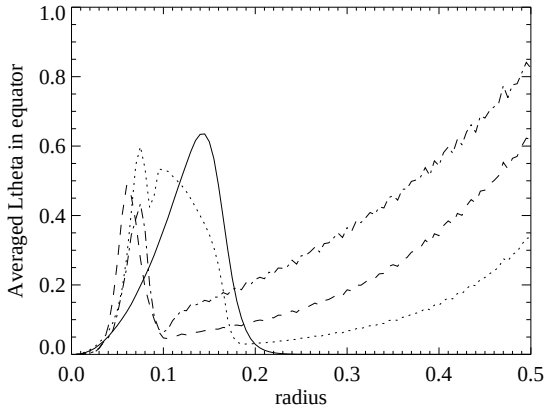

Figure 5.21: Angular momentum per unit mass, averaged over circular cells, on the equatorial plane. The timesteps are 0 (solid line), 500 (dotted line), 1000 (dashed line) 1500 (dashed-dotted line)

central core, we end up with four smaller cores that rotate around their center of mass.

5.4 Comparison with previous works

Although this latter experiment's results seem strange, we must note that *similar results were obtained by previous studies*. Simulations of gravitational collapse of a uniform sphere, rotating as a solid body, were made by R.B. Larson (1972) with the use of a 2D numerical code. He found that after the initial flattening of the density distribution, "centrifugal forces in the central part of the cloud begin to exceed gravity and collapse perpendicular to the axis of rotation is halted near the center. Meanwhile, collapse along the axis of rotation continues unimpeded until nearly all of the material near the axis has fallen into the core. After that, the central density stops increasing and even begins to decrease as the material rebounds outward in the equatorial plane. At the same time, material from the outer part of the cloud continues to fall inward and accumulate in *a ring-shaped region around the periphery of the center*. The density builds up rapidly in this region, while the central density continues to decrease so that the density distribution begins to resemble a "doughnut" with a density minimum at the center. Once such a "doughnut" or ring has begun to form, its gravitational attraction draws more material into it and the ring becomes steadily more massive and condensed". Larson finds the formation of such a ring in nearly all of his experiments not surprising, since a flattened rotating disk is subject to numerous instabilities (actually an equilibrium disk was never really formed). He suggests that since this ring structure is highly

unstable, the ultimate outcome will most probably be the fragmentation into a binary or multiple system of condensations orbiting around each other and he proposes that this could be the mechanism for the formation of multiple systems of stars, which is the most common case in the universe. Our current results appear to be in full agreement with Larson's description of such a collapse.

In addition, Black and Bodenheimer (1976) came to very similar conclusions based on experiments made with a 2D hydrodynamical code. They describe the collapse as split into 5 distinct phases: 1) the initial flattening of the cloud, 2) the formation of an axisymmetric ring-like structure in the inner part of the cloud, 3) a brief equilibrium phase of the ring, 4) the ring collapse upon itself, where it begins to contract under the influence of its self-gravity and 5) an ejection of a high velocity "sheet" of material from the outer periphery of the ring. After this latter phase they stop their simulations since numerical errors become crucial. Our experiment is consistent with the first four stages. We did not observe such an ejection of material, but as they suggest, this effect could actually be a numerical artifact, or it could be due to lack of angular momentum transport mechanisms, such as viscosity, in their equations. They also note that if this is the case, then the likely post-equilibrium ring evolution is the fragmentation into two or more condensations, just like Larson suggested. Our results support this suggestion. Finally, note that in both cases, the "angular momentum problem is resolved, since much of the cloud's initial angular momentum either goes to the orbital motion of the condensations or it is transported outward through the ejection of the sheet of gas.

There are however, more recent experiments with highly sophisticated numerical codes, such as those of Abel, Bryan and Norman (2001), that take into account many more factors and have come up with only one single central core. They argue, that the idea of such a multiple system formation is the effect of unrealistic initial conditions like the ones used in this simulation and those mentioned above. They also suggest that many details of the collapse forming a primordial star are determined by the properties of the hydrogen molecule. It should be mentioned though, that our aim is not to simulate a fully realistic collapse of a primordial gas cloud, but rather to examine the gravitational collapse of relatively simple initial gas spheres.

One more conclusion that seems quite safe to deduce from the previous experiments is that there is a tendency for specific angular momentum to accumulate in as small a volume as possible. In the experiments with the small resolution, almost all of the angular momentum is stored on a disk which has a small radius around the center (smaller than the theoretically predicted one) and therefore it rotates rapidly. A very small amount is carried by particles near the boundaries. On the higher resolution, latter experiment, the angular momentum is more efficiently transferred outwards and the fraction that is stored in the disk and then piled into the ring eventually creates instabilities that fragment the ring. Finally, all the angular momentum that had not yet been driven out, is carried by even smaller structures, the four gas clumps. As a conclusion one can assume that a system whose angular momentum is distributed in a big volume of mass, is unstable and will probably evolve towards a state where its

total angular momentum will be carried by as small volumes of mass as possible. Note though that this does not necessarily mean that it will be carried away from the cloud. The latter experiment shows that although large amounts of L are being driven outwards, the rest is still crucial in determining the fate of the collapse.

Therefore we can conclude that the issue of how angular momentum is being redistributed while collapse is occurring is a very complicated one and although the initial cloud is a simple structure, its final state is sensitive to how much angular momentum will be efficiently transported outwards, and how the rest of it will be distributed in the cloud.

5.5 Conclusions

The conclusions that can be reached from the first experiment are:

- A disk is once again formed, as expected.
- The disk's mass and self-gravity are not negligible. Actually more mass is left rotating than in the core although theoretically we expected the opposite.
- The inner parts of the disk *do* become Keplerian but only for a brief period of time. It is those parts that remain orbiting until the end of the simulation.
- The accretion rate is far from constant. It is also totally different from Boss and Black's (1982) figure.
- Most of the cloud's angular momentum is stored in the disk and is not sufficiently transported outwards throughout the simulation.

From the second experiment we can deduce that:

- The low resolution and the periodic boundaries are significantly affecting the collapse. By confining the cloud in a small grid box we seem to promote a specific evolution. When we move to higher resolution and allow the cloud to expand freely, a different evolution is observed.
- Pressure forces and mass accumulation around the core can become crucial and *do* play a major role in the collapse.
- The disk that forms can be highly unstable and can lead to the formation of a ring structure which, being unstable as well, fragments into a systems of spherical clumps.
- Therefore *a single central core is not the only possible outcome* of an axisymmetric collapse. A multiple system of cores can arise.

- This evolution is much more efficient in transporting angular momentum outwards. The rest is transformed into orbital angular momentum of the multiple cores.

Chapter 6

Non Uniform Rotation

So far, we have studied the collapse of a non rotating singular isothermal sphere, of a rotating one and of a uniform density rotating sphere. One common aspect that all these models share, is that they have a very simple, symmetric, initial density and velocity profile. Their density distributions were either: $\rho \propto r^{-2}$ or $\rho = \rho_0$ which are simple, spherically symmetric distributions of mass for all radii. In the rotating cases, the cloud initially rotates as a rigid body, which simplifies the theoretical analysis very much, since the collapsing particles' trajectories don't intersect, thus allowing us to apply ballistic orbits in order to study them analytically.

As a result, all the cases follow, more or less, a similar collapse, where the inner shells collapse quickly and so does the material close to the rotational axis, creating a core, while the layers that initially carried a lot of angular momentum settle on a flattened surface on the equatorial plane, which rotates around the core, i.e. a rotating disk. This disk is unlikely to find a stable Keplerian profile and be able to retain it for more that a few timesteps, as more material settles on it, rearranging its structure and redistributing its mass and angular momentum.

Yet, if one wants to approach more realistic models of collapse, closer to the interstellar gas clouds and starformation processes observed in the universe, he should examine much more complex systems. The protostellar clouds could not have such simple density profiles, where one power law describes their mass distribution throughout their whole radius. It is also naive to assume that all their spherical cells could be in such high coordination as to rotate with the same angular velocity around a common axis.

It is closer to reality to imagine a protostellar cloud as a system of spherical cells that have different mass distributions, different rotations, and certainly different rotational axes. These models are expected to follow a much more complicated gravitational collapse than the ones already described.

Hence, in an effort to approach such an intrinsic collapse, we made an experiment with the 3D stagger code where a slightly more complicated initial condition was implemented. This last case is not studied as thoroughly as the other ones, but serves as a good example of what new features of collapse may

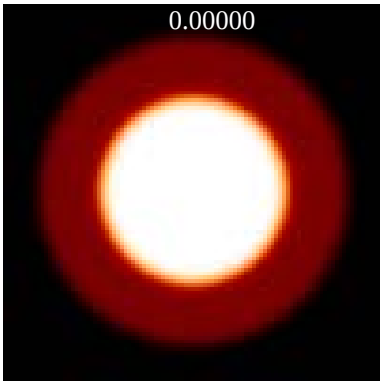

Figure 6.1: The cloud is composed of two spherical concentric layers. The inner one has density $\rho = 1$ and a vertical rotational axis, while the outer one has $\rho = 2$ and a horizontal axis. Timestep=0

be expected.

Once again we use a 100x100x100 grid box, in the center of which we implement a spherical cloud that is made up of two different concentric spherical layers. The inner one has a uniform density: $\rho = 1$ and is rotating around a rotational axis that coincides with the z axis, with $\Omega = 6.333$. The outer layer has uniform density $\rho = 2$ and rotates with angular velocity $\Omega = 12.666$ around a rotational axis, perpendicular to that of the inner layer. The code ran for 2000 timesteps.

The collapse is depicted in Figures 6.1 to 6.7. The physical, scaled time is shown in each one. In the first timesteps they collapse into a bar structure, which quickly contracts to form two spherical clumps rotating around each other that soon merge into one elongated structure. One remarkable phenomenon is that *two* disks are soon formed, one perpendicular to the other. These two disks, not exactly flat nor symmetric around the center, compose this final structure that appears to roughly retain its shape for most of the timesteps. The two disks are shown in Figure 6.8 where the density isosurface $\rho = 4$ is plotted. One of them, corresponding to the inner cell, is *growing in size* while the other is *gradually being absorbed*.

The whole structure is loosing large amounts of mass continuously, as gas is being ejected with great velocities, mostly from the two edges of the elongated cloud while some material is landing on it. Apparently these edges have the lowest gravitational energy since they are away from the cloud's center, and the

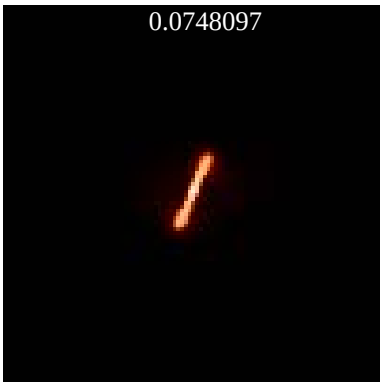

Figure 6.2: Timestep=250

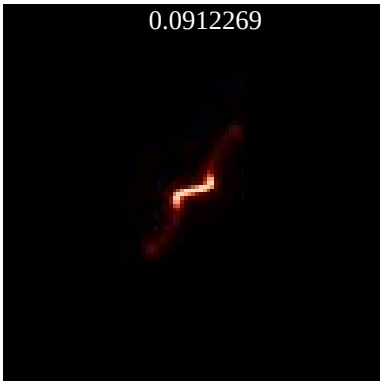

Figure 6.3: Timestep=500

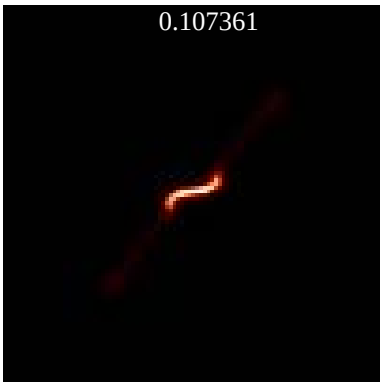

Figure 6.4: Timestep=750

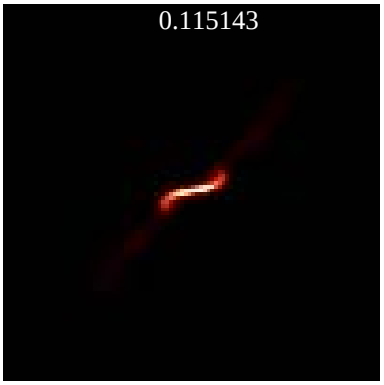

Figure 6.5: Timestep=1000

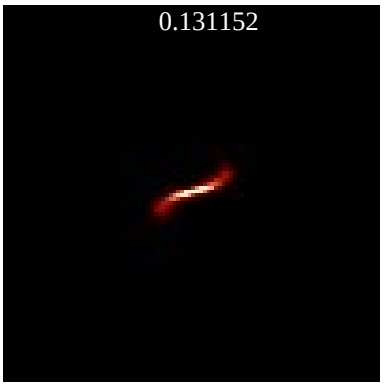

Figure 6.6: Timestep=1250

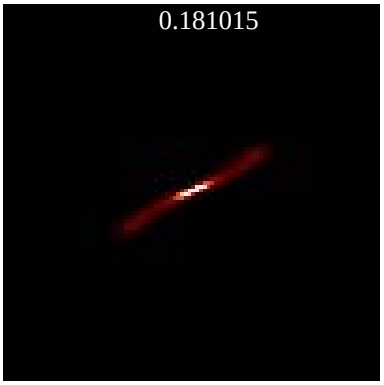

Figure 6.7: Timestep=2000

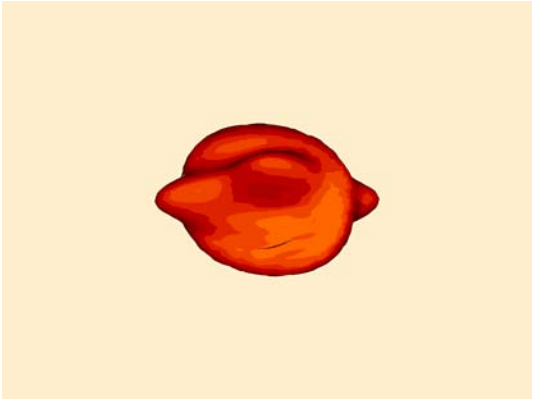

Figure 6.8: 3D density isosurface ($\rho = 4$) where the two disks are visible. Timestep=400

highest rotational energies since the whole structure is rotating. Therefore, the particles with the highest values of angular momentum are leaving the cloud, releasing large amounts of rotational energy from it, allowing it to settle in a more stable shape. These mass jets are occurring during the whole run, increasing and dropping every few timesteps. Close to the center, gravity is enough to make the inner parts contract and create a single core. By the end of the experiment, mass was still being ejected towards the boundaries, while the inner parts where slowly accumulating closer to the center.

We can therefore see that, even when we apply a model that is only very slightly more complicated, the evolution is much different and more complex. Although some general features of rotating collapse (that prove unavoidable) are seen here as well, like the formation of disk-like structures, one for each axis of rotation, the detailed evolution is completely different. So, we can conclude that the simple models studied above are just very rough approximations of real collapse. They can provide a general idea about some basic features that will probably be encountered in a realistic collapse, (like the disk or the core formation), but under no circumstance should they be considered fair descriptions of real clouds' collapse.

We point out once more that the way angular momentum is being redistributed in all the gas throughout the collapse is also very complicated. In the latter experiment we observed large jets of mass that carry angular momentum along, but the central structure was still unstable and rotating, and every few timesteps it was releasing new amounts of gas on its surroundings. It is therefore quite naive to accept the simple theoretical model of angular momentum transport, analyzed earlier, and expect that most of the mass will end up in a central core leaving only a very tiny fraction, rotating at great distances, carrying the initial angular momentum.

Chapter 7

Discussion

Six experiments have been presented and analyzed in this report.

First we studied the gravitational collapse of a singular isothermal sphere and two simulations were done for that purpose. A sink cell was applied in the first one and most results were close to the theoretical ones, verifying to a certain degree the self-similar solution developed by Shu (1977). The second simulation did not have a sink cell in the core and this time the results were different. Basic features of the self-similar collapse, such as the free-fall profile and the steady accretion rate were not observed at all.

We then run a simulation where the singular isothermal sphere was set into solid body rotation. The outcome was compared with the available theory but was not found to be in agreement. Although a rotating disk was formed, its structure and evolution was not what we expected. The infalling gas did not have the expected density distributions as well and the accretion rate was far from steady. This disagreement is probably caused by the fact that in the theoretical analysis many simplifying assumptions were made, unlike the numerical experiment.

Further on, we studied the collapse of a spherical cloud with uniform initial density and solid body rotation. It was found that a rotating disk was once again formed and even became quasi-Keplerian for a short period of time. The amount of material that was still orbiting around the center by the end of the simulation was much larger than what previous works had suggested and it appears that angular momentum was not sufficiently transported outwards. Since a lot of material was initially ejected and bounced at the boundaries, we performed the same experiment in a bigger grid-box where the cloud had enough space to expand freely. This time the collapse follows a completely new path, where a disk is formed only to be soon followed by the formation of a ring, which after a stabilized period breaks down to spherical clumps, rotating around the center. This procedure appears to be much more efficient in angular momentum transport. Results such as those are supported by some previous studies and indicate a possible path to multiple core formation.

Finally we ended this series of experiments with the simulation of a more

complex cloud, where two uniform density profiles and two rotations are combined. This last simulation presents completely new features of collapse, such as jets of mass and an elongated core, not observed in the previous, simple cases, but also retains basic other ones, such as the disk formation.

From the above experiments and their analysis, we can reach some final, basic conclusions:

- The use of a sink-cell in the core is very helpful in deducing elegant, analytical solutions, but may not be realistic. The core can grow considerably in size, and the pressure forces around it may influence the collapse to a great extent.

- The fact that a purely free-fall collapse was not observed indicates that pressure forces in general play an important role in all cases, and can alter the expected result very much. They should not be neglected when dealing with gravitational collapse.

- A disk *always* appears in the rotating cloud experiments, even with more intricate initial conditions and multiple rotational axes. It accumulates large amounts of mass, so that its self-gravity should not be neglected. It seems unlikely that it will ever reach a stable, Keplerian, rotation profile and be able to retain it long enough.

- When the cloud has enough space to freely expand and evolve, without the tight confinement of boundaries, it follows a very different and more involved path.

- The same happens when we implement even slightly more complicated initial conditions. A new type of evolution is obtained.

- One common feature in all previous experiments with rotation, both simple and complex ones, is that actually *a lot of mass* is left out of the core, in order to carry the cloud's angular momentum. As a result the final core has much less mass that the theoretically predicted one. We would like to point out that the subject of angular momentum redistribution is still open to further and more sophisticated analysis, in order to approach a more realistic model that will be capable of making a fair prediction of the evolution of a collapsing cloud.

Finally it must be emphasized that all the experiments discussed here, even the last one, have extremely simplified initial conditions and should not be considered as true and faithful representations of the gravitational collapse observed during starformation in the universe. Yet they can serve as rough guidelines which indicate some basic features of collapse. They also indicate that it is essential to make numerical simulations in three dimensions, as they are much closer to reality than the symmetric 1D or 2D ones and can offer a more complete insight to starformation.

Bibliography

[1] *Accretion Processes in Star Formation*, Lee Hartmann, Cambridge University Press

[2] *Star Formation*, International Astronomical Union Symposium No. 75, T. De Jong & A. Maeder, D. Reidel Publishing Company, 1977

[3] Stone J. M., Balbus S. A., 1996, Ap. J., 464, 364

[4] Balbus S. A., Hawley J. F., 1991, Ap. J., 376, 214

[5] Laughlin G., Bodenheimer P., 1994, Ap. J., 436, 335

[6] Larson R. B., 1972, M.N.R.A.S., 156, 437

[7] Black D. C., Bodenheimer P., 1976, Ap. J., 206, 138

[8] Lynden-Bell D., Pringle J. E., 1974, M.N.R.A.S., 168, 603

[9] Boss A. P., Black D. C., 1982, Ap. J., 258, 270

[10] Shu F. H., 1977, Ap. J., 214, 488

[11] Cassen P., Moosman A., 1981, Icarus, 48, 353

[12] Tereby S., Shu F. H., Cassen P., 1984, Ap. J., 286, 529

[13] Abel T., Bryan G. L., Norman M. L., 2002, The formation of the first star in the universe, Draft version

All H.S.T. images were aquired from the website:
http://hubblesite.org/gallery